

Sorption of Thorium Onto Subsurface Geomedia

by

Nathan Hunter Melson

A thesis submitted to the Graduate Faculty of
Auburn University
in partial fulfillment of the
requirements for the Degree of
Master of Science

Auburn, Alabama
December 12, 2011

Copyright 2011 by Nathan Hunter Melson

Approved by

Mark O. Barnett, Chair, Malcolm Pirnie Professor of Civil Engineering
Prahbakar Clement, Arthur H. Feagin Professor of Civil Engineering
Dongye Zhao, Huff Professor of Civil Engineering

Abstract

Radionuclide contamination has been a significant environmental problem at US Department of Energy (USDOE) sites for many years. In addition, a final disposal solution for radioactive waste, such as deep geological repositories, has also been a topic of investigation in recent years due to the high volume of waste held at surface interim facilities. In this paper, sorption characteristics of Th(IV) onto several geomedia were investigated using batch techniques. Thorium has been used as an analog for other tetravalent actinides such as U(IV) and Pu(IV) since actinides of the same oxidation state exhibit similar chemical behavior. The sorption of Th(IV) has been shown to be strong adsorbate due to its tendency to hydrolyze readily.

Multiple batch experiments were performed to evaluate the sorption properties of Th(IV) onto several geomedia in the presence of carbonate. The geomedia used in these studies included two subsurface sediments from the USDOE Savannah River site: a sandy sediment (SRSS) and clayey sediment (SRSC) and two minerals: goethite and kaolinite. These studies showed that sorption of Th(IV) was strong (>95%) for pH 3.5-10 for both SRSS, SRSC, and goethite at a total carbonate concentration of 0.01 M. Th(IV) sorption onto kaolinite was strong for pH 2-5, but sorption decreased from pH 5 to 11. For a total carbonate concentration of 0.1 M, sorption decreased significantly for SRSS from pH 6 to 12 and decreased slightly for SRSC from pH 9 to 11.

Precipitation of Th(IV) oxides was also tested in conjunction with these sorption studies. These tests showed that precipitation had a significant role in removal of aqueous Th(IV) from solution at the Th(IV) concentration used. Further investigations indicated the formation of “true” Th(IV) colloids in the absence of geomeia and pseudo-colloids in the presence of geomeia.

These studies concluded that as carbonate concentration increases, Th(IV) sorption decreases at near neutral and alkaline pH values. Although sorption of Th(IV) is strong in the same pH range at lower carbonate concentrations, it may be in the form of surface precipitation onto colloids. Thus, the formation of these pseudo-colloids can actually increase the mobility of contaminants.

Acknowledgements

The author would like to express his gratitude for the wonderful guidance and support of his advisor Dr. Mark Barnett. The author would also like to thank his other committee members Dr. Prabhakar Clement, Dr. Dongye Zhao, and the rest of the environmental faculty in the civil engineering department for their instruction, knowledge, and support during the author's time at Auburn University.

Furthermore, The author would like to thank Jinling Zhuang for his technical assistance and support in the environmental laboratory at Auburn University. The author would especially like to thank Brian Haliena for his assistance with experiments and other work in the laboratory. Finally, I would like to thank my family and friends who supported me throughout my studies here at Auburn University. This research was supported by the Office of Science (BER), U. S. Department of Energy.

Table of Contents

Abstract	ii
Acknowledgements	iv
List of Tables	vii
List of Figures	viii
Chapter 1. Introduction	1
1.1 Problem Statement	1
1.2 Objectives	3
1.3 Organization	4
Chapter 2. Literature Review	5
2.1 Radionuclide Contamination	5
2.2 Thorium Health Concerns	6
2.3 General Thorium Chemistry and Mineralogy	7
2.4 Speciation of Thorium	8
2.5 Solubility of Thorium Oxides	12
2.6 Sorption of Thorium onto Geomedia	16
Chapter 3. Sorption of Thorium onto Subsurface Geomedia	19
3.1 Introduction	19

3.2 Materials and Methods.....	20
Materials.....	20
Experimental Methods.....	21
Modeling.....	23
3.3 Results and Discussion.....	23
Speciation of Th in aqueous systems.....	23
Th(IV) Kinetics.....	23
Th(IV) Isotherm.....	28
Th(IV) Precipitation.....	28
Formation Th(IV) Pseudo-colloids.....	34
Th(IV) Sorption onto SRSS.....	37
Th(IV) Sorption onto SRSC.....	37
Th(IV) Sorption onto Goethite.....	41
Th(IV) Sorption onto Kaolinite.....	43
Effect of Carbonate on Th(IV) Sorption.....	46
Chapter 4. Conclusions and Recommendations for Future Work.....	52
4.1 Conclusions.....	52
4.2 Recommendations for Future Work.....	54
References.....	55
Appendix.....	60

List of Tables

Table 2.1: Thorium hydrolysis reactions occurring at $T=25^{\circ}\text{C}$ and $I=0.0\text{ M}$ and associated $\log K$ values. $\log K$ constants were calculated from thermodynamic data given by (Rand, Fuger et al. 2008).....	9
Table 2.2: Thorium carbonate reactions occurring at $T=25^{\circ}\text{C}$ and $I=0.0\text{ M}$ and associated $\log K$ values. $\log K$ constants were calculated from thermodynamic data given by (Rand, Fuger et al. 2008).....	11
Table 2.3: Thorium solubility reactions occurring at $T=25^{\circ}\text{C}$ and $I=0.0\text{ M}$ and associated $\log K_{\text{sp}}$ values. $\log K_{\text{sp}}$ constants were calculated from thermodynamic data given by (Rand, Fuger et al. 2008).....	14
Table 3.1: SRS Soil Characterization (Kaplan, 2010).....	21

List of Figures

Figure 2.1: Th(IV) speciation diagram calculated using Visual MINTEQ. $C_{\text{Th}}=3.35 \times 10^{-5} \text{ M}$, $I=0.1 \text{ M NaNO}_3$	10
Figure 2.2: Th(IV) speciation diagram calculated using Visual MINTEQ. $C_{\text{Th}}=3.35 \times 10^{-5} \text{ M}$, $I=0.09 \text{ NaNO}_3/0.01 \text{ M NaHCO}_3$	11
Figure 2.3:Th(IV) speciation diagram calculated using Visual MINTEQ. $C_{\text{Th}}=3.35 \times 10^{-5} \text{ M}$, $I=0.1 \text{ M NaHCO}_3$	12
Figure 2.4: Theoretical solubility edges for ThO_2 (am, fresh), ThO_2 (am, aged), and $\text{ThO}_2(\text{s})$, which were calculated using Visual MINTEQ with values from (Rand, Fuger et al. 2008); $I=0.09 \text{ M NaNO}_3/0.01 \text{ M NaHCO}_3$	15
Figure 2.5: Theoretical solubility edges for ThO_2 (am, fresh), ThO_2 (am, aged), and $\text{ThO}_2(\text{s})$, which were calculated using Visual MINTEQ with values from (Rand, Fuger et al. 2008); $I=0.1 \text{ M NaHCO}_3$	16
Figure 3.1: Th(IV) speciation diagram calculated using Visual MINTEQ. $C_{\text{Th}}=3.35 \times 10^{-5} \text{ M}$, $I=0.1 \text{ M NaNO}_3$	24
Figure 3.2: Th(IV) speciation diagram calculated using Visual MINTEQ. $C_{\text{Th}}=3.35 \times 10^{-5} \text{ M}$, $I=0.09 \text{ NaNO}_3/0.01 \text{ M NaHCO}_3$	25
Figure 3.3: Th(IV) speciation diagram calculated using Visual MINTEQ. $C_{\text{Th}}=3.35 \times 10^{-5} \text{ M}$, $I=0.1 \text{ M NaHCO}_3$	26
Figure 3.4: Equilibrium kinetics of Th(IV) with SRSS at $m/V = 3.33 \text{ g/L}$, $C_0=3.08 \times 10^{-5} \text{ M}$, $I=0.10 \text{ M NaNO}_3$, $\text{pH}=4.15\pm 0.09$, $\text{Temp}=26\pm 1 \text{ }^\circ\text{C}$	27
Figure 3.5: Adsorption Isotherm of Th(IV) onto SRSS; $I=0.10 \text{ M NaNO}_3$, $\text{pH}=4.13\pm 0.04$, $\text{Temp}=26\pm 1 \text{ }^\circ\text{C}$	29
Figure 3.6: % Th(IV) Dissolved vs. pH for samples containing no soil compared to the theoretical solubility curves of $\text{ThO}_2(\text{am, fresh})$ $\text{ThO}_2(\text{am, aged})$. $C_0(\text{Th(IV)}) = 3.31 \times 10^{-5} \text{ M}$, $I=0.09 \text{ M NaNO}_3/0.01 \text{ M NaHCO}_3$, $\text{Temp}=26\pm 1 \text{ }^\circ\text{C}$	30

Figure 3.7: Dissolved Th(IV) concentrations vs. pH for $C_{\text{TCO}_3}=0.01$ M compared to the theoretical solubility for ThO_2 (am, fresh) and ThO_2 (am, aged), which were calculated using Visual MINTEQ and values from (Rand, Fuger et al. 2008); $C_0=3.31 \times 10^{-5}$ M; $I=0.09$ M $\text{NaNO}_3/0.01$ M NaHCO_3 , $T=26\pm 1$ °C 31

Figure 3.8: Th(IV) concentration as a function of Th(IV) particle size removed from solution by centrifugation. $\text{pH}=4.34\pm 0.08$, $C_0=3.40 \times 10^{-5}$ M, $I=0.1$ M NaNO_3 , $\text{Temp.}=26\pm 1$ °C. Dotted line shows the solubility threshold of ThO_2 (am, aged). 33

Figure 3.9: Th(IV) concentration vs. SRSS particle size at $m/V=3.31$, $C_0=3.05 \times 10^{-5}$, $I=0.1$ M NaNO_3 , $\text{pH}=4.19\pm 0.04$, $\text{Temp}=26\pm 1$ °C..... 36

Figure 3.10: % Th(IV) Dissolved vs. pH for different m/V s of SRSS. $C_0(\text{Th(IV)}) = 3.34 \times 10^{-5}$ M, $I=0.09$ M $\text{NaNO}_3/0.01$ M NaHCO_3 , $\text{Temp}=26\pm 1$ °C..... 38

Figure 3.11: % Th(IV) Dissolved vs. pH for different m/V s of SRSC. $C_0(\text{Th(IV)}) = 3.30 \times 10^{-5}$ M, $I=0.09$ M $\text{NaNO}_3/0.01$ M NaHCO_3 , $\text{Temp}=26\pm 1$ °C..... 39

Figure 3.12: % Th(IV) Dissolved vs. pH for different solid-solution ratios of goethite. $C_0(\text{Th(IV)}) = 3.34 \times 10^{-5}$ M, $I=0.09$ M $\text{NaNO}_3/0.01$ M NaHCO_3 , $\text{Temp}=26\pm 1$ °C.... 42

Figure 3.13: % Th(IV) Dissolved vs. pH for different m/V s of kaolinite. $C_0(\text{Th(IV)}) = 3.34 \times 10^{-5}$ mol/L, $I=0.09$ M $\text{NaNO}_3/0.01$ M NaHCO_3 , $\text{Temp}=26\pm 1$ °C..... 44

Figure 3.14: Dissolved Th(IV) concentrations vs. pH for for different m/V s of kaolinite compared to the theoretical solubility for ThO_2 (am, fresh) and ThO_2 (am, aged), which were calculated using Visual MINTEQ and values from (Rand, Fuger et al. 2008); $C_0=3.34 \times 10^{-5}$ M; $I=0.09$ M $\text{NaNO}_3/0.01$ M NaHCO_3 , $T=26\pm 1$ °C 45

Figure 3.15: % Th(IV) Dissolved vs. pH at $C_{\text{TCO}_3}=0.1$ M; $C_0=3.40 \times 10^{-5}$ mol/L, $I=0.1$ M NaHCO_3 , $\text{Temp.}=26\pm 1$ °C. Results for samples containing no geomeedia are compared with theoretical solubility curves for ThO_2 (am, fresh) and ThO_2 (am, aged). 48

Figure 3.16: Dissolved Th(IV) concentrations vs. pH for $C_{\text{TCO}_3}=0.1$ M compared to the theoretical solubility for ThO_2 (am, fresh) and ThO_2 (am, aged), which were calculated using Visual MINTEQ; $C_0=3.34 \times 10^{-5}$ M; $I=0.1$ M NaHCO_3 , $T=26\pm 1$ °C 49

Figure 3.17: % Th(IV) Dissolved vs. pH for SRSS at $C_{\text{TCO}_3}=0.1$ M; $C_0=3.40 \times 10^{-5}$ mol/L, $I=0.1$ M NaHCO_3 , $\text{Temp.}=26\pm 1$ °C. Experimental results at SRSS concentrations of 0.49 g/L (\diamond) and 16.33 g/L (Δ) compared to samples

containing no geomeia (X) and the theoretical solubility curves for ThO₂ (am, fresh) (dashed line) and ThO₂ (am, aged) (solid line)..... 50

Figure 3.18: % Th(IV) Dissolved vs. pH for SRSC at C_{TCO3}=0.1 M; C₀=3.40 x 10⁻⁵ mol/L, I=0.1 M NaHCO₃, Temp.=26±1 °C. Experimental results at SRSC concentrations of 0.49 g/L (◇) and 16.41 g/L (Δ) compared to samples containing no geomeia (X) and the theoretical solubility curves for ThO₂ (am, fresh) (dashed line) and ThO₂ (am, aged) (solid line)..... 51

Chapter 1.

Introduction

1.1 Problem Statement

Since the 1940s, substantial amounts of radionuclides have since been dispersed into the atmosphere and biosphere due to the detonations of nuclear weapons, spills from nuclear processing facilities, and improper disposal practices. In addition to these environmental incidents, the final disposal method for nuclear waste has become a cause for investigation due to the high volume of waste held at interim storage facilities. For over 20 years, one of the proposed solutions has been to build nuclear waste repositories deep underground to store the waste for tens of thousands to millions of years (Vasicek and Svoboda 2011). The goal of this disposal method is to delay the release of radionuclides to the biosphere until their radiological impact is negligible (Kim, Kwon et al. 2011). However, there is the possibility of the waste containers deteriorating before the nuclear waste decays sufficiently, allowing the waste to seep into the environment. Therefore, the study of the fate and transport of different radionuclides is necessary for researchers to prevent or mitigate a contaminant release into the local soil and groundwater.

In past decades, iron oxides, such as goethite (α -FeOOH(s)), have been investigated as a sorbent for radionuclides since metal containers have been used in the past as an initial barrier in nuclear waste storage. According to the Cornell and

Schwertmann (2003), goethite is the second most common iron oxide and the most common in iron rust. This makes goethite an extremely important sorbent to help mitigate the release of radioactive waste into the environment since many waste containers are made of steel (Rojo, Seco et al. 2009). Other barriers used to slow the release and migration of radioactive waste includes solidifying waste with concrete (Duffo, Farina et al. 2010), lining the storage area with concrete, and using certain types of soils or clays as backfills (Schmeide and Bernhard 2010). One such clay that is common in many soils and backfills is kaolinite (Banik, Buda et al. 2007). Kaolinite has been investigated in several sorption studies of different actinides, which have shown to sorb strongly to the clay (Banik, Buda et al. 2007; Buda, Banik et al. 2008; Schmeide and Bernhard 2010). Natural soils have also been shown to be strong sorbents for actinides (Powell, Robert et al. 2002). Also, different soil properties including pH and organic matter can affect the mobility and bioavailability of actinides (Guo, Duan et al. 2008).

Therefore, it is necessary to understand the interactions between soils and minerals and radionuclides such as thorium. For many years, the sorption of thorium onto a wide variety of sorbents has been studied. Thorium has been listed as priority contaminant at US Department of Energy (USDOE) sites for many years (ATSDR 2009). Actinide elements such as Th, U, Np, and Pu, tend to exhibit similar chemical characteristics when the elements are in the same oxidation state. Because of its stable tetravalent oxidation state, Th(IV) has been used as an analog for other a tetravalent actinides such as U(IV), Np(IV), and Pu(IV) (Choppin 1999; Banik, Buda et al. 2007; Buda, Banik et al. 2008), which can be difficult to maintain in their

tetravalent oxidation state. Furthermore, actinides in their +IV oxidation states have been shown to be less soluble and thus less mobile than +V or +VI oxidation states (Runde 2000). Because of its high oxidation state, Th tends to form hydroxide complexes readily. These Th-hydroxo complexes have shown strong sorption characteristics onto many different types of geomeia (Laflamme and Murray 1987; Righetto, Bidoglio et al. 1988; Osthols 1995; Cromieres, Moulin et al. 1998; Jakobsson 1999; Powell, Fjeld et al. 2004; 2005; Reiller, Casanova et al. 2005; Rojo, Seco et al. 2009).

In addition to adsorption of Th onto geomeia, surface precipitation also plays a role in the migration of Th in aqueous subsurface environments. Due to the low solubility of Th oxides, amorphous Th precipitates may form in solution and adhere to soil and mineral surfaces (Yun, Kim et al. 2006). Soil and mineral particles that are of most concern from a contaminant transport perspective are colloids. Colloids, which range in size from 1 nm to 1 μm , can greatly enhance the movement of adsorbed or surface-precipitated contaminants due to their large specific surface area and ability to move through the interstitial area in subsurface environments (Cromieres, Moulin et al. 1998).

1.2 Objectives

The main objectives of this thesis are to 1) determine the ability of natural sediments from the Savannah River Site and synthetic minerals to remove Th(IV) in subsurface environments and 2) to investigate the effects of carbonate concentration on Th(IV) sorption and precipitation. Batch experiments were

utilized to determine the sorption characteristics for each geomeia and how increased carbonate concentration affected Th(IV) sorption and precipitation.

1.3 Organization

The organization of this report follows the guidelines for a publication-style thesis as outlined in the *Guide to Preparation and Submission of Theses and Dissertations* by the Auburn University Graduate School. A literature review is given in Chapter 2. The materials, methods, and results from the batch experiments are discussed in Chapter 3. Chapter 3 is a draft manuscript, which will be submitted later for publication in a peer-reviewed scientific journal. Chapter 4 contains the conclusions from these studies as well as future recommendations for future studies.

Chapter 2.

Literature Review

2.1 Radionuclide Contamination

Since the 1940s, substantial amounts of radionuclides have since been dispersed into the atmosphere and biosphere due to the detonations of nuclear weapons, spills from nuclear power facilities, and improper disposal practices at U.S. Department of Energy (USDOE) manufacturing facilities. In the United States, much of the uranium and plutonium was produced for use in nuclear weapons and were manufactured on USDOE sites such as the Savannah River Site and Hanford Site (Delistraty and Yokel 1999; Mathes and Rasmussen 2006). In recent years, the focus of these sites has shifted from the production of nuclear materials to environmental cleanup since both of the sites have been on the National Priorities List (NPL) by the U.S. Environmental Protection Agency (EPA) in the late 1980s (USEPA 2011).

Another topic of concern for scientists and government agencies is the final disposal method for nuclear waste. For over 20 years, one of the accepted solutions to this problem has been to build nuclear waste repositories deep underground to store the waste for tens of thousands to millions of years (Kim, Kwon et al. 2011). This method would allow some of the nuclear waste time to decay into their nonradioactive daughter products and is thought to be far enough away from

human activity to prevent any accessibility from humans. However, there is the possibility of the waste containers deteriorating before the nuclear waste decays allowing the waste to seep into the environment. Therefore, the study of the fate and transport of different radionuclides is necessary to prevent or mitigate a contaminant release into the local soil and groundwater systems. The elements that are of environmental concern are those that have long half-lives such as Thorium-232 [Th(IV)], Uranium-238 and Plutonium-239, which have half-lives in millions to billions of years. Thorium has been listed as a hazardous substance for many years and is a known carcinogen (ATSDR 2011). Thorium has also been used as an analog for other tetravalent actinides since it has a stable tetravalent oxidation state (Altmaier, Neck et al. 2005). There is also the concern that Th(IV) contamination may increase in the future due to the renewed interest for use of Th(IV) as a nuclear fuel (Rojo, Seco et al. 2009).

2.2 Thorium Health Concerns

Thorium is a radioactive metal that is naturally present in the earth's crust and can be found worldwide at low concentrations in water, rocks, soils, and air, and as a result found in plants and animals (USEPA 2011). The average concentration of Th(IV) in soils is approximately six parts per million (ppm) (ATSDR 2011). Thorium is most commonly found at higher concentrations in the environment as part of the phosphate mineral monazite (ThPO_4) (Peterson, MacDonell et al. 2007). The Agency for Toxic Substances & Disease Registry (ATSDR) ranked Th(IV) at 101 on its CERCLA Priority List of Hazardous Substances (LHS), which shows that thorium is not the foremost concern at facilities on the National Priorities List (NPL) (ATSDR

2009). Thorium is registered by the EPA and ASTDR as a known carcinogen and has been shown to increase the risk of several cancers including lung and bone cancers (ATSDR 2011; USEPA 2011). Thorium is considered mildly radioactive due to its extremely long half-life ($t_{1/2}$ = 14 billion years). When it does decay, Th(IV) emits an alpha particle, which can be harmful depending on a person's proximity to the particle. However, these health risks are significantly reduced as long as Th(IV) particulates are not ingested or inhaled. The EPA's maximum contaminant level (MCL) for radionuclides such as Th(IV) in drinking water is 8 pCi/L or 7.3 $\mu\text{g-Th/L}$ (using the specific activity of Th-232 = 1.1×10^{-7} Ci/g) (Peterson, MacDonell et al. 2007; USEPA 2011).

2.3 General Thorium Chemistry and Mineralogy

In its metallic form Th(IV) is a soft, ductile, silvery-white in color and has a density similar to lead. When heated, Th(IV) will burn a bright white, which made it an ideal product to be used in lantern mantles. Since it has a half-life of 14 billion years, more than 99% of Th(IV) occurring in the environment is Th-232 and is stable in its tetravalent oxidation state (Peterson, MacDonell et al. 2007). Monazite (ThPO_4) is the primary mineral ore containing Th(IV) (6 to 7% by weight), whereas Thorite (ThSiO_4) is the most prevalent Th(IV) mineral (72% by weight) (Freidman 2011).

Actinide chemistry can be quite complex because some actinides can exist in multiple oxidation states in the same system (Choppin 2007). Nonetheless, actinides tend to exhibit similar properties when they are in the same oxidation state. Because of its stability in the tetravalent oxidation state, Th(IV) has been studied as

an analog for other tetravalent actinides such as U(IV) (Rai, Felmy, et al. 1997), Np(IV), and Pu(IV) (Altmaier, Neck et al. 2005; Guo, Yu et al. 2005; Chang, Yu et al. 2007; Choppin 2007). This technique is advantageous because it simplifies the research process by removing any redox reactions that may occur with other actinides. However, Choppin (2007) suggests that some corrections or adjustments should be made to data when using Th(IV) as an analog for Pu(IV). These adjustments are attributed to the ionic radii being relatively smaller, which makes Th(IV) complexation somewhat weaker (Choppin 2006).

2.4 Speciation of Thorium

The speciation of an element is the distribution of that element among the chemical species in a system. An analysis of the speciation of an element is extremely important when trying to model the behavior of that element such as solubility, toxicity, adsorption to soils, and the surface properties of solids. Several processes can be used to detect the different Th(IV) species including potentiometric titrations, laser-induced breakdown detection, and various spectroscopy methods (Choppin 2007).

When metal ions complex with water molecules, a reaction called hydrolysis occurs where a proton is transferred from the hydrated metal to water forming hydroxo complexes. Since Th(IV) is stable in a tetravalent oxidation state in solution, it has a remarkable ability to form monomeric and polymeric hydroxide complexes. Numerous studies have been done over the years to determine the formation constants of Th(IV) hydroxides in various media. The most common anions in media used to study Th(IV) hydrolysis are perchlorate (Baes, Meyer et al. 1965; Grenthe

and Lagerman 1991; Ekberg, Albinsson et al. 2000), nitrate (Milic 1971; Brown, Ellis et al. 1983), and chloride (Baes and Mesmer 1981; Milic 1981). The OECD Nuclear Energy Agency (NEA) reviewed and summarized all the relevant literature, and the hydroxide species and their constants with the most consistent results are shown in Table 2.1 (Rand, Fuger et al. 2008). Using these values from Table 2.1, a Th(IV) speciation diagram was completed as shown in Figure 2.1 using the equilibrium speciation software Visual MINTEQ. Figure 2.1 shows that there are only five major hydroxide complexes present in the system. The ionic form, Th^{4+} , predominating at $\text{pH} < 3.2$, ThOH^{3+} from $\text{pH} 3.2$ to $\text{pH} 4.1$, $\text{Th}_4(\text{OH})_{12}^{4+}$ dominating from $\text{pH} 4.1$ to $\text{pH} 7.8$, and $\text{Th}(\text{OH})_4(\text{aq})$ at $\text{pH} > 7.8$.

Table 2.1: Thorium hydrolysis reactions occurring at $T=25^\circ\text{C}$ and $I=0.0\text{ M}$ and associated log K values. Log K constants were calculated from thermodynamic data given by (Rand, Fuger et al. 2008).

Species	Th(IV) Hydroxide Complexation Reactions	Log K
$\text{Th}(\text{OH})^{3+}$	$\text{Th}^{4+} + \text{H}_2\text{O}(\text{l}) \leftrightarrow \text{H}^+ + \text{Th}(\text{OH})^{3+}$	-2.500
$\text{Th}(\text{OH})_2^{2+}$	$\text{Th}^{4+} + 2\text{H}_2\text{O}(\text{l}) \leftrightarrow 2\text{H}^+ + \text{Th}(\text{OH})_2^{2+}$	-6.200
$\text{Th}(\text{OH})_4(\text{aq})$	$\text{Th}^{4+} + 4\text{H}_2\text{O}(\text{l}) \leftrightarrow 4\text{H}^+ + \text{Th}(\text{OH})_4(\text{aq})$	-17.400
$\text{Th}_2(\text{OH})_2^{6+}$	$2\text{Th}^{4+} + 2\text{H}_2\text{O}(\text{l}) \leftrightarrow 2\text{H}^+ + \text{Th}_2(\text{OH})_2^{6+}$	-5.900
$\text{Th}_2(\text{OH})_3^{5+}$	$2\text{Th}^{4+} + 3\text{H}_2\text{O}(\text{l}) \leftrightarrow 3\text{H}^+ + \text{Th}_2(\text{OH})_3^{5+}$	-6.800
$\text{Th}_4(\text{OH})_8^{8+}$	$4\text{Th}^{4+} + 8\text{H}_2\text{O}(\text{l}) \leftrightarrow 8\text{H}^+ + \text{Th}_4(\text{OH})_8^{8+}$	-20.400
$\text{Th}_4(\text{OH})_{12}^{4+}$	$4\text{Th}^{4+} + 12\text{H}_2\text{O}(\text{l}) \leftrightarrow 12\text{H}^+ + \text{Th}_4(\text{OH})_{12}^{4+}$	-26.600
$\text{Th}_6(\text{OH})_{14}^{10+}$	$6\text{Th}^{4+} + 14\text{H}_2\text{O}(\text{l}) \leftrightarrow 14\text{H}^+ + \text{Th}_6(\text{OH})_{14}^{10+}$	-36.800
$\text{Th}_6(\text{OH})_{15}^{9+}$	$6\text{Th}^{4+} + 15\text{H}_2\text{O}(\text{l}) \leftrightarrow 15\text{H}^+ + \text{Th}_6(\text{OH})_{15}^{9+}$	-36.800

When considering natural systems, one of the most important areas in water chemistry is the carbonate system. The carbonate system mainly consists of gaseous CO_2 , $\text{CO}_{2(\text{g})}$, aqueous CO_2 , $\text{CO}_{2(\text{aq})}$, carbonic acid, H_2CO_3 , bicarbonate, HCO_3^- , and carbonate, CO_3^{2-} (Snoeyink and Jenkins 1980). Similarly, carbonate complexation

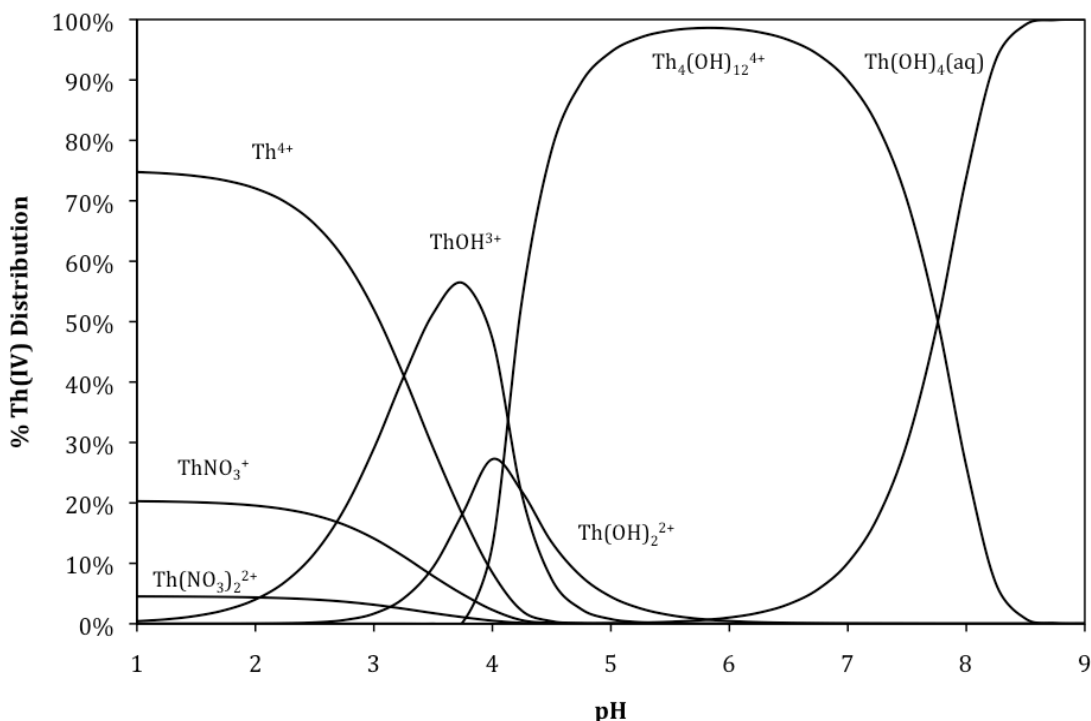


Figure 2.1: Th(IV) speciation diagram calculated using Visual MINTEQ. $C_{tTh}=3.35 \times 10^{-5}$ M, $I=0.1$ M NaNO₃.

with thorium is also a very important part of aqueous actinide systems. Some studies used CO_{2(g)} at different partial pressures to provide the carbonate in solution (Osthols, Bruno et al. 1994; Felmy, Rai et al. 1997; Altmaier, Neck et al. 2005; Altmaier, Neck et al. 2006), and others used a HCO₃⁻/CO₃²⁻ buffer solution with total carbonate concentrations ranging from 0.001 to 2.3 (Felmy, Rai et al. 1997; Altmaier, Neck et al. 2005; Altmaier, Neck et al. 2006). The OECD NEA (Rand, Fuger et al. 2008) reviewed and summarized these articles and selected the species shown in Table 2.2 because they had the most reliable quantitative data. Figure 2.2 and Figure 2.3 show the distribution of Th(IV) species in the presence of carbonate at total carbonate concentrations of 0.01 M and 0.1 M, respectively. When compared to Th(IV) complexation with hydroxide, there isn't much differentiation in species distribution until after pH 6.5. At this point ternary Th(IV) hydroxide-carbonate

species begin to become the more dominant species for the remainder of the pH range with the exception of $\text{ThOH}_4(\text{aq})$, which becomes dominant at $\text{pH} > 10.5$.

Table 2.2: Thorium carbonate reactions occurring at $T=25^\circ\text{C}$ and $I=0.0\text{ M}$ and associated log K values. Log K constants were calculated from thermodynamic data given by (Rand, Fuger et al. 2008).

Species	Th(IV) Carbonate Complexation Reactions	Log K
$\text{Th}(\text{CO}_3)_5^{6-}$	$\text{Th}^{4+} + 5\text{CO}_3^{2-} \leftrightarrow \text{Th}(\text{CO}_3)_5^{6-}$	31.000
$\text{ThOH}(\text{CO}_3)_4^{5-}$	$\text{Th}^{4+} + \text{H}_2\text{O}(\text{l}) + 4\text{CO}_3^{2-} \leftrightarrow \text{H}^+ + \text{ThOH}(\text{CO}_3)_4^{5-}$	21.600
$\text{Th}(\text{OH})_2(\text{CO}_3)_2^{2-}$	$\text{Th}^{4+} + 2\text{H}_2\text{O}(\text{l}) + 2\text{CO}_3^{2-} \leftrightarrow 2\text{H}^+ + \text{Th}(\text{OH})_2(\text{CO}_3)_2^{2-}$	8.800
$\text{Th}(\text{OH})_4(\text{CO}_3)^{2-}$	$\text{Th}^{4+} + 4\text{H}_2\text{O}(\text{l}) + \text{CO}_3^{2-} \leftrightarrow 4\text{H}^+ + \text{Th}(\text{OH})_4(\text{CO}_3)^{2-}$	-15.600

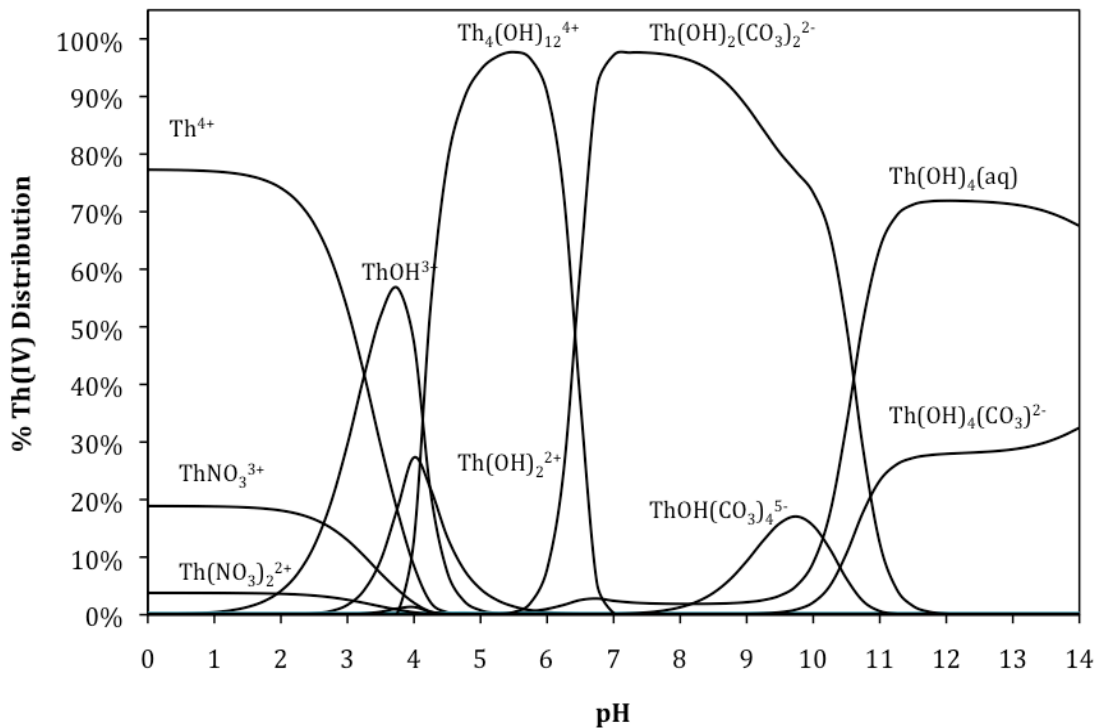


Figure 2.2: Th(IV) speciation diagram calculated using Visual MINTEQ. $C_{\text{Th}}=3.35 \times 10^{-5}\text{ M}$, $I=0.09\text{ NaNO}_3/0.01\text{ M NaHCO}_3$

2.5 Solubility of Thorium Oxides

Solubility is of great importance to the fate and transport of contaminants. Many factors affect the solubility of a substance including temperature, pressure, the nature of the substance being dissolved (e.g., polarity, size of solid, etc.), and experimental procedures (e.g., stirring, pretreatment, etc.). Like all chemical systems that are at constant temperature and pressure, reactions take place in order to minimize the total Gibb's free energy. When the Gibb's free energy is at a minimum the chemical reaction is considered to be at equilibrium. When describing the dissolution of a solid in a liquid, the equilibrium constant is called the solubility product, K_{sp} .

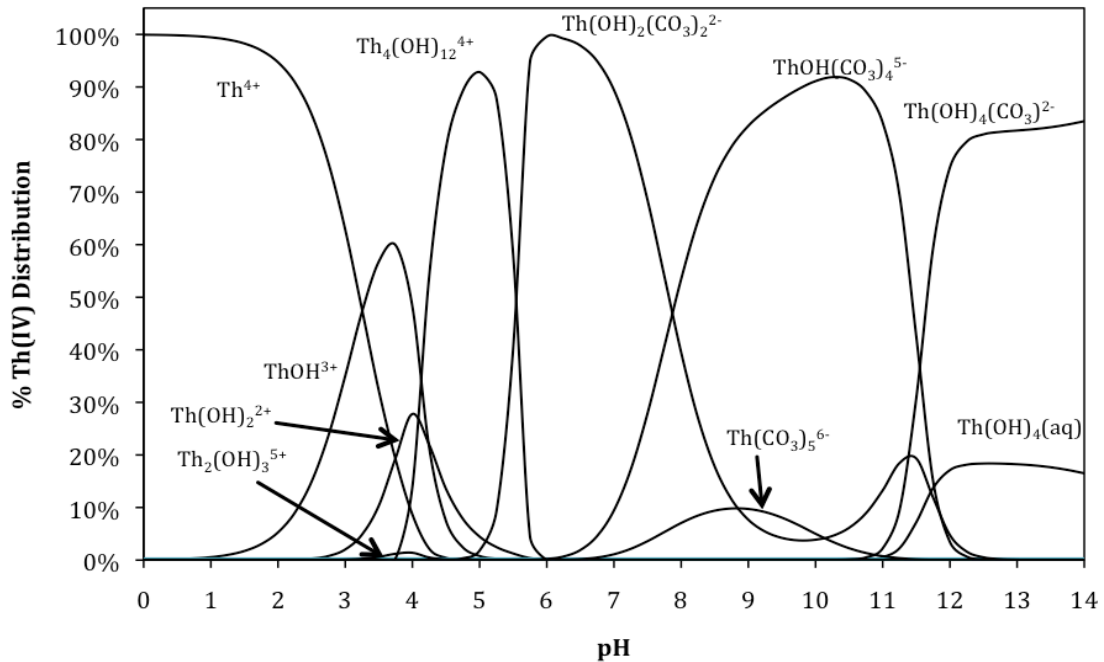
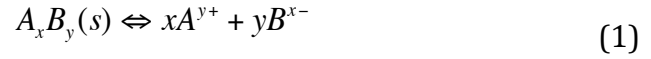


Figure 2.3: Th(IV) speciation diagram calculated using Visual MINTEQ. $C_{tTh} = 3.35 \times 10^{-5}$ M, $I = 0.1$ M $NaHCO_3$

For the general equation,



The solubility product is

$$K_{sp} = \frac{\{A^{y+}\}^x \{B^{x-}\}^y}{\{A_x B_y (s)\}} = [A^{y+}]^x [B^{x-}]^y \{\gamma_{A^{y+}}\}^x \{\gamma_{B^{x-}}\}^y \quad (2)$$

where $\{i\}$ indicates activity and $[i]$ indicates concentration, and γ_i is the activity coefficient of species i . Over the years there have been many studies concerning the solubility of Th(IV) oxides and hydroxides. Most of these solubility studies were conducted using the undersaturation approach, where the thorium solid was placed into a solution and allowed to equilibrate (Ryan and Rai 1987; Osthols, Bruno et al. 1994; Felmy, Rai et al. 1997; Altmaier, Neck et al. 2004; Kim, Baik et al. 2010). As thorium begins to precipitate in solution, the solid is considered either an amorphous hydroxide, $\text{Th}(\text{OH})_4(\text{am})$, or a microcrystalline hydrous oxide $\text{ThO}_2 \cdot x\text{H}_2\text{O}(\text{am})$ (Neck and Kim 2000). (Rai, Moore et al. 2000) reports that after some time $\text{ThO}_2(\text{am})$ transforms into the less soluble crystalline thorium oxide, $\text{ThO}_2(\text{cr})$. The amount of time for $\text{ThO}_2(\text{am})$ to transform into the crystalline solid decreases as the temperature of the solution increases (270 days at 25°C and about 12 days at 100°C) (Neck and Kim 2001). (Neck and Kim 2001) state that water-free $\text{ThO}_2(\text{cr})$ requires heating the solids to temperatures greater than 700°C. After reviewing this information, as $\text{ThO}_2(\text{am})$ aged the solubility decreased and two solubility constants were selected for the amorphous solid: $\text{ThO}_2(\text{am}, \text{fresh})$ and $\text{ThO}_2(\text{am}, \text{aged})$. Rand, Fuger et al. (2008) acknowledged that there isn't a definite time when $\text{ThO}_2(\text{am}, \text{fresh})$ becomes $\text{ThO}_2(\text{am}, \text{aged})$. Still, The suggested

equilibration times used to differentiate between ThO₂(am, fresh) and ThO₂(am, aged) are <25 days and >70 days, respectively (Rand, Fuger et al. 2008). The solubility products for these two solids and crystalline ThO₂ are shown in Table 2.3. Log solubility plots for the three solids at different carbonate concentrations are shown in Figure 2.4 and Figure 2.5.

Table 2.3: Thorium solubility reactions occurring at T=25°C and I=0.0 M and associated log K_{sp} values. Log K_{sp} constants were calculated from thermodynamic data given by (Rand, Fuger et al. 2008).

Th(IV) Solubility Reactions	Log K _{sp}
Th⁴⁺ + 2H₂O(l) ↔ 4H⁺ + ThO₂ (am, fresh)	-9.300
Th⁴⁺ + 2H₂O(l) ↔ 4H⁺ + ThO₂ (am, aged)	-8.500
Th⁴⁺ + 2H₂O(l) ↔ 4H⁺ + ThO₂(s)	-1.766

Even though thorium solubility has been extensively studied for many years, discrepancies still exist about solubility constants. The solubility of the two thorium oxide solids differs by about 7 orders of magnitude under acidic conditions, but as the solution becomes neutral and alkaline the solubility data for both solids became similar (Neck, Altmaier et al. 2003). (Neck, Altmaier et al. 2003) concluded in this study that bulk ThO₂(cr) must be covered with an amorphous surface layer or be infused with ThO₂(am). Equilibrium thermodynamics assert that the solubility values should continue to be different even at neutral pH. In order to test this phenomenon, (Vandenborre, Abdelouas et al. 2008) decided to conduct a study on the interaction of the solid interface of ThO₂(cr). Although the results of this study were not entirely conclusive, the presence of thorium colloids may be precipitating onto the bulk ThO₂(cr) surface. The formation of Th(IV) colloids has been accepted

and studied by several researchers and may help explain the discrepancies in Th(IV) solubility constants (Neck and Kim 2001; Neck, Muller et al. 2002; Bitea, Muller et al. 2003; Yun, Kim et al. 2006).

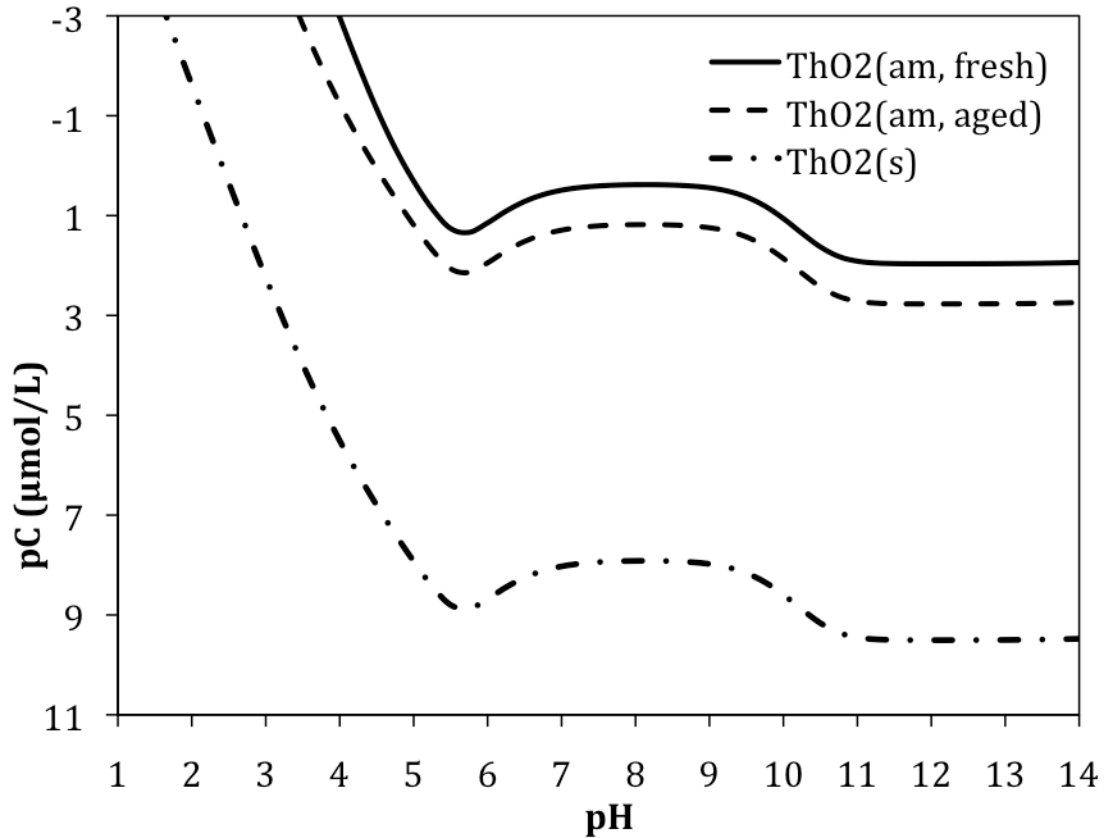


Figure 2.4: Theoretical solubility edges for ThO₂ (am, fresh), ThO₂ (am, aged), and ThO₂(s), which were calculated using Visual MINTEQ with values from (Rand, Fuger et al. 2008); I=0.09 M NaNO₃/0.01 M NaHCO₃.

Colloidal formation is also of major importance to understand the migration of actinides in subsurface environments since colloids enhance the transportability of a contaminant due to the nature of their size (Degueldre and Kline 2007). Thorium colloidal migration is typically in the form of pseudo-colloids where Th(IV) solids precipitate onto aquatic colloids (Yun, Kim et al. 2006).

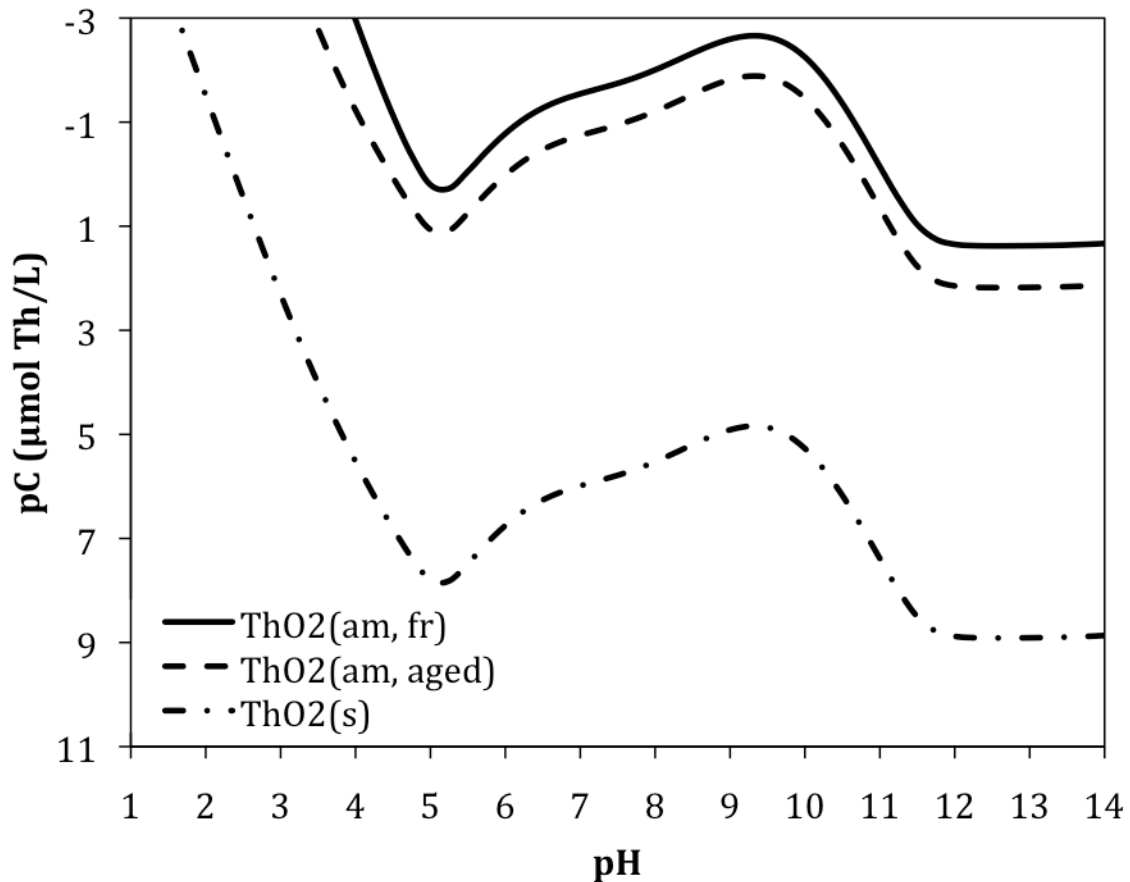


Figure 2.5: Theoretical solubility edges for ThO₂ (am, fresh), ThO₂ (am, aged), and ThO₂(s), which were calculated using Visual MINTEQ with values from (Rand, Fuger et al. 2008); I=0.1 M NaHCO₃.

2.6 Sorption of Thorium onto Geomedia

There have been numerous studies on the sorption of Th(IV) in environmental systems. In recent years, many of these studies were conducted in response to the growing need of radioactive waste repositories around the world. Due to its use as an analog for other tetravalent actinides as well as being listed on the CERCLA LHS, Th(IV) sorption has been studied on many different types of geomedia. Thorium typically shows strong sorption characteristics because of its inclination to hydrolyze readily. Iron oxides have been shown to generate reducing

environments thereby causing multivalent actinides to stay in their less mobile tetravalent state (Powell, Fjeld et al. 2004; 2005). Because of their abundance in the earth's crust and the proximity to radioactive waste, i.e. the waste container, several Th(IV) sorption studies have been done on iron oxides and oxyhydroxides including magnetite and ferrihydrite (Rojo, Seco et al. 2009; Seco, Hennig et al. 2009), hematite (Cromieres, Moulin et al. 1998; Murphy, Lenhart et al. 1999; Reiller, Moulin et al. 2002; Reiller, Casanova et al. 2005), and goethite (Laflamme and Murray 1987; Hunter, Hawke et al. 1988).

Several studies involve Th(IV) sorption onto other oxides consisting of silica (Osthols 1995; Osthols, Manceau et al. 1997; Chen and Wang 2007), alumina (Righetto, Bidoglio et al. 1988; Guo, Niu et al. 2005; Chen and Wang 2007), or titania (Jakobsson 1999; Guo, Niu et al. 2005; Tan, Wang et al. 2007). Most of these sorbents were used as they also exhibit low solubility and ubiquity in nature. (Li and Tao 2002) carried out a comparative study on Th(IV) sorption onto alumina and silica and found their sorption characteristics to be similar. Furthermore, there have been only a couple studies on the sorption of Th(IV) onto some common clay minerals such as kaolinite, which is considered a component of many soils and contains hydroxylated sites of silicon and aluminum (Banik, Buda et al. 2007; Buda, Banik et al. 2008). Sorption of Th(IV) onto kaolinite was very strong with about 85% of Th(IV) adsorbed at pH=1.

A key issue associated with most studies conducted in a laboratory is how well the results will correlate to in real-world environmental systems. Since there have been numerous releases of radioactive waste in the past at the SRS facility,

(Powell, Robert et al. 2002) conducted a study on plutonium sorption on soil obtained from SRS. In this study four natural SRS burial ground sediments were used as sorbents: surface sandy sediment, surface clayey sediment, subsurface sandy sediment, and subsurface clayey sediment. Batch experiments were conducted to examine the sorption edges for these sediments with Pu(IV) and Pu(V). Plutonium(IV) sorbed strongly (>95%) to each sediment at low pH values (pH<3), while Pu(V) achieved >95% sorbed at approximately pH 5.5. It was also shown that after 33 days the sorption edge for Pu(V) was similar to the sorption edge for Pu(IV) at 0 days, which indicated that Pu(V) was being reduced to Pu(IV) by these sediments.

Another component to consider in natural systems that can complicate thorium sorption is natural organic matter, specifically humic substances (HS). Humic substances are not a specific chemical species but rather a macromolecular colloidal phase (Chang, Yu et al. 2007). Humic substances are generally classified into three separate fractions: (1) humin, the insoluble fraction; (2) humic acids, which are soluble about pH>3.5; and (3) fulvic acids, which are soluble at all pH values (Chang, Yu et al. 2007). Studies have shown that at low pH HSs improve Th(IV) sorption onto mineral surfaces, has little effect on sorption at intermediate pH, and can reduce sorption at high pH values (Chang, Yu et al. 2007; Tan, Wang et al. 2007; Fan, Wu et al. 2008).

Chapter 3.

Sorption of Thorium onto Subsurface Geomedia

This chapter serves as a draft manuscript. It will later be submitted for publication in a peer-reviewed scientific journal article.

3.1 Introduction

The subject of sorption of thorium (Th(IV)) onto different geomedia has been studied extensively. Thorium has been shown to adsorb strongly to minerals such as iron oxides (Laflamme and Murray 1987; Hunter, Hawke et al. 1988; Cromieres, Moulin et al. 1998; Murphy, Lenhart et al. 1999; Rojo, Seco et al. 2009), clays such as kaolinite (Banik, Buda et al. 2007; Buda, Banik et al. 2008), and some natural Savannah River Site (SRS) soils (Powell, Robert et al. 2002). However, few studies have investigated the effects of carbonate concentration on Th(IV) sorption onto geomedia such as goethite, kaolinite, and SRS soils. The objectives of this study were to 1) determine the ability of natural sediments from the SRS, synthetic goethite and kaolinite to remove Th(IV) in subsurface environments and 2) to investigate the effects of carbonate concentration on Th(IV) sorption and precipitation.

3.2 Materials and Methods

Materials

For this research, four different geomedia were used: two natural soils from the Savannah River Site (SRS), kaolinite clay, and synthetic crystalline goethite. The SRS soils were subsurface sand (SRSS) and subsurface clay (SRSC). The soil characteristics are shown in Table 3.1.

The SRSS and SRSC samples were sieved to remove particles greater than 2 mm. The SRSC was also gently homogenized using a mortar and pestle. No other pretreatment was used on the SRSS and SRSC. The kaolinite was obtained from EMD Chemicals, Inc. Pure crystalline goethite was synthesized in house via rapid hydrolysis of 1 M Fe(III) nitrate salt as previously described by Schwertmann and Cornell (2000) and Loganathan et al. (2009). Following the hydrolysis step, the product was slowly heated under highly alkaline conditions (ca. pH 12), which was maintained by 5 M KOH. At a set oven temperature of 65°C, maintained for about 60 hours, the blood-red colored amorphous ferrihydrite ($\text{Fe}_2\text{O}_3 \cdot 0.5 \text{H}_2\text{O}$) precipitated during the hydrolysis step turned into ocher-colored goethite precipitate. The precipitate was placed in dialysis tubing (MWCO 2000) and suspended in a deionized water bath for approximately one week. The supernatant was then decanted and the pure goethite was freeze dried and used in the experiments.

Chemicals used in this study were all certified ACS grade from VWR International LLC or Fisher Scientific, and solutions were prepared with double-deionized water prepared with a Milli-Q system. The Th(IV) stock solution was prepared by dissolving solid $\text{Th}(\text{NO}_3)_4 \cdot 4\text{H}_2\text{O}$, which was obtained from International

Bio-Analytical Industries Inc., in 0.07 M HNO₃. Thorium standards were prepared by diluting a Th(IV) atomic absorption standard from Sigma-Aldrich.

Table 3.1: SRS Soil Characterization (Kaplan, 2010).

Soil	Subsurface Clay	Subsurface Sand
% sand (>53 μm)	57.9	97
% silt (53 – 2 μm)	40.6	2.9
% clay (<2 μm)	1.6	0.2
Textural classification	Silty clay	Sand
pH	4.55	5.1
% OM	8.8	0
CEC (cmol/kg)	1.09 ± 0.31	-0.35 ± 0.22
AEC (cmol/kg)	1.58 ± 0.61	0.06 ± 0.19
BET surface area (m ² /g)	15.31	1.27
Single point surface area (m ² /g)	15.07	1.24
CDB extractable Fe (mg/g)	15.26	7.06
Al (ppm)	63.59	16.64
Na (ppm)	42.91	34.69
Mg (ppm)	144.05	98.76
Ca (ppm)	64.41	24.62
K (ppm)	182.87	92.97
Mineralogy	Kao > goeth > Hem (no qtz or 14 A)	Kao > goeth > musco/14A (no qtz)

Experimental Methods

Batch adsorption experiments were conducted using 50-mL Teflon, polycarbonate, or polypropylene centrifuge tubes sealed with screw caps under ambient conditions (25±1° C and atmospheric pressure). Each tube generated one data point. Duplicates were used in most experiments to show reproducibility. Each sample was prepared as follows: an appropriate amount of geomeia was added to each tube, then using calibrated pipettes, a background solution (NaNO₃, NaNO₃/NaHCO₃, or NaHCO₃) was added, followed by the Th(IV) stock solution, and finally HNO₃ or NaOH to adjust pH. All background solutions and NaOH and HNO₃

were freshly prepared before each experiment. Samples were prepared rapidly and capped tightly to reduce the exchange of CO₂ with the atmosphere.

Each sample was placed into an end-over-end tumbler that rotated at approximately 4 rpm for 48 hours. After being removed from the tumbler, the samples were immediately tested for pH using a pH meter and combination electrode (Thermo Orion Model 410 A+). Each sample was centrifuged for 30 minutes at 8000 rpm (8880 xg), which removed soil and ThO₂ particles 74 and 32 nm in size, respectively, to separate the solid phase from the liquid phase.

A portion of the supernatant of each sample was placed into a corresponding secondary vial and acidified to 0.1 M HNO₃. Each of these solutions were shaken and allowed to equilibrate for approximately 30 minutes before being analyzed. A Varian 710-ES ICP-OES was used to analyze the concentration in each of the Th(IV) solutions. The amount of Th(IV) sorption was calculated from the difference between the initial concentration and the equilibrated concentration. Solid phase concentrations were calculated as follows,

$$q_e = \frac{(C_0 - C_e) \cdot V}{1000 \cdot m}$$

where q_e is the Th(IV) uptake concentration (mg-Th/g-soil), C_0 is the initial Th(IV) aqueous concentration (mg-Th/L), C_e is the equilibrium Th(IV) aqueous concentration (mg-Th/L), V is the total volume in the sample (mL), and m is the mass of the soil added to the sample (g).

Modeling

In modeling our experimental data, we used the equilibrium speciation model Visual MINTEQ with thermodynamic data from (Rand, Fuger et al. 2008). All aqueous Th(IV) reactions and corresponding stability constants that were used in our research are shown in Table 2.1, 2.2, and 2.3.

3.3 Results and Discussion

Speciation of Th in aqueous systems

Using the values from Table 2.1 and 2.2, the distribution of Th in aqueous solutions for different carbonate concentrations is shown in Figure 3.1, 3.2, and 3.3. For solutions without any carbonate in the system, Th^{4+} is the dominant species for $\text{pH} < 3$. At $\text{pH} > 3$, the formation of Th hydroxide species ThOH^{3+} , $\text{Th}(\text{OH})_2^{2+}$, $\text{Th}_4(\text{OH})_{12}^{4+}$, and $\text{Th}(\text{OH})_4(\text{aq})$ is observed with increasing pH. In contrast, with increasing carbonate concentration, negatively charged ternary Th-hydroxide-carbonate complexes become the predominant species for the $\text{pH} = 6.5\text{-}10.5$ ($C_{\text{TCO}_3} = 0.01 \text{ M}$) and $\text{pH} > 5.5$ ($C_{\text{TCO}_3} = 0.1 \text{ M}$).

Th(IV) Kinetics

In order to determine the amount of time needed for samples to reach equilibrium, a kinetics test was conducted using SRSS as the geomedia. The results of this test are shown in Figure 3.4. Results from statistical t-tests indicated that there was not a significant difference ($p < 0.05$) in dissolved Th(IV) concentrations between 24 and 48 hours, yet there was an observable difference as shown on

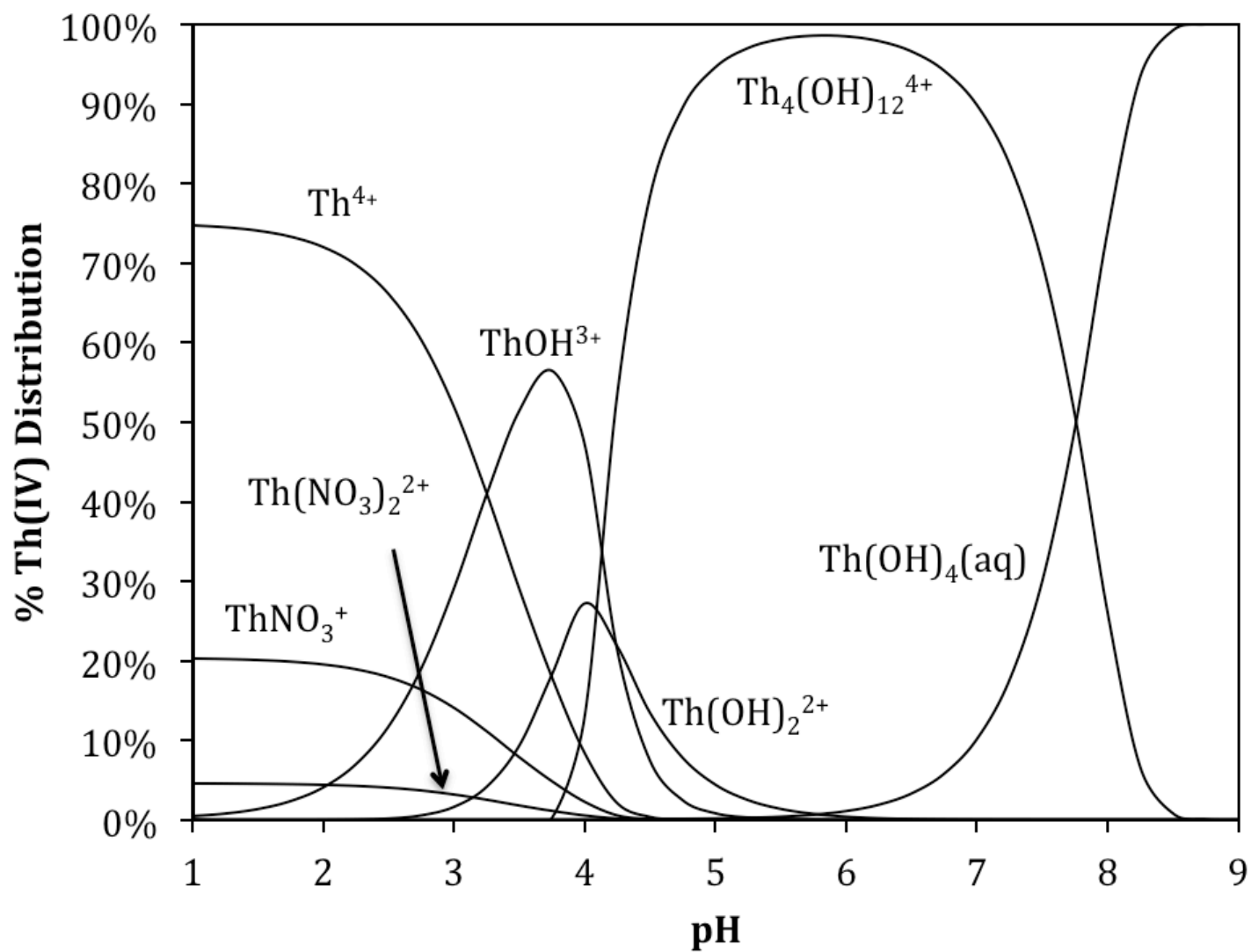


Figure 3.1: Th(IV) speciation diagram calculated using Visual MINTEQ. $C_{\text{Th}}=3.35 \times 10^{-5}$ M, $I=0.1$ M NaNO_3 .

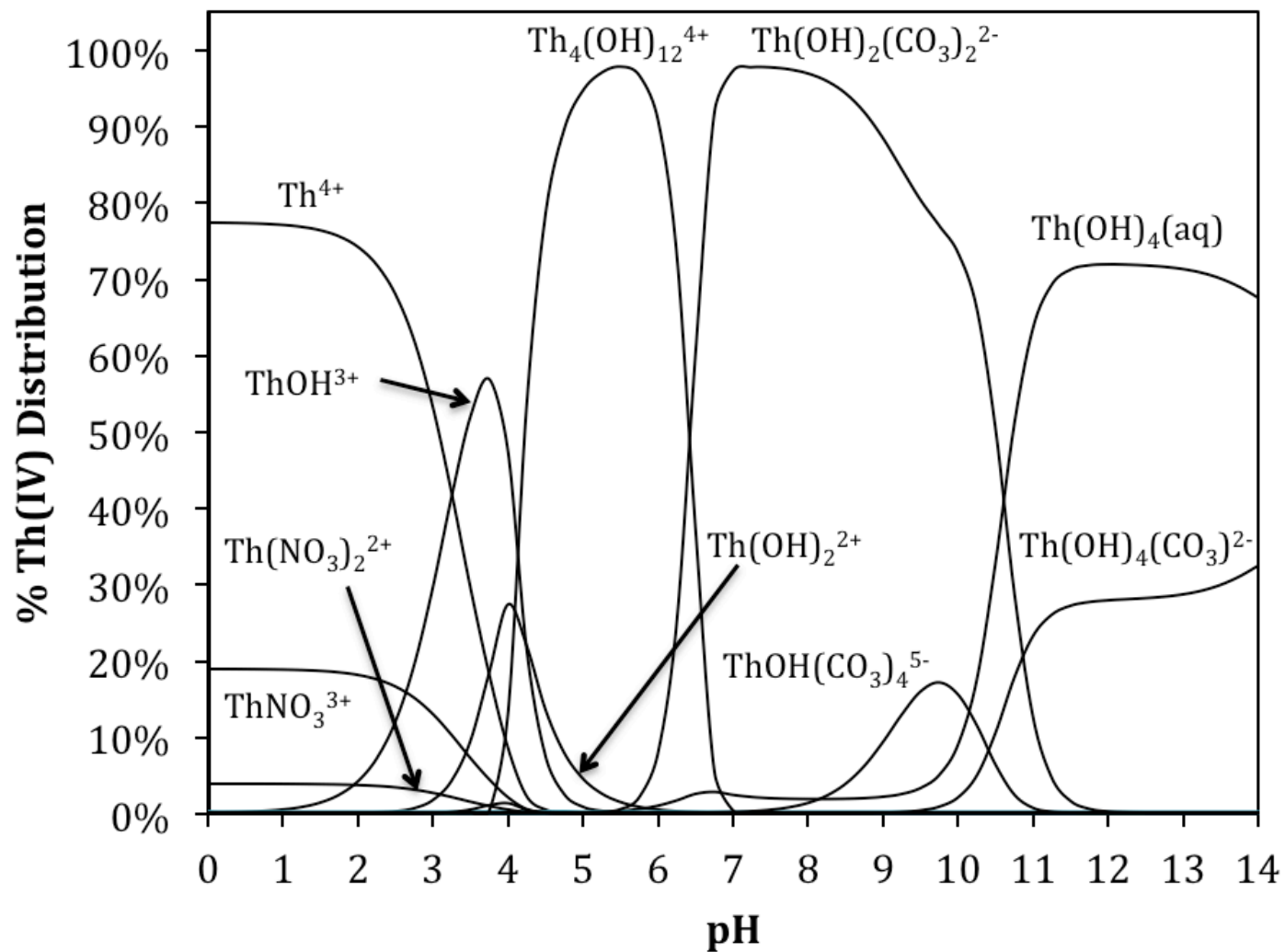


Figure 3.2: Th(IV) speciation diagram calculated using Visual MINTEQ. $C_{\text{Th}} = 3.35 \times 10^{-5}$ M, $I = 0.09$ NaNO₃/0.01 M NaHCO₃.

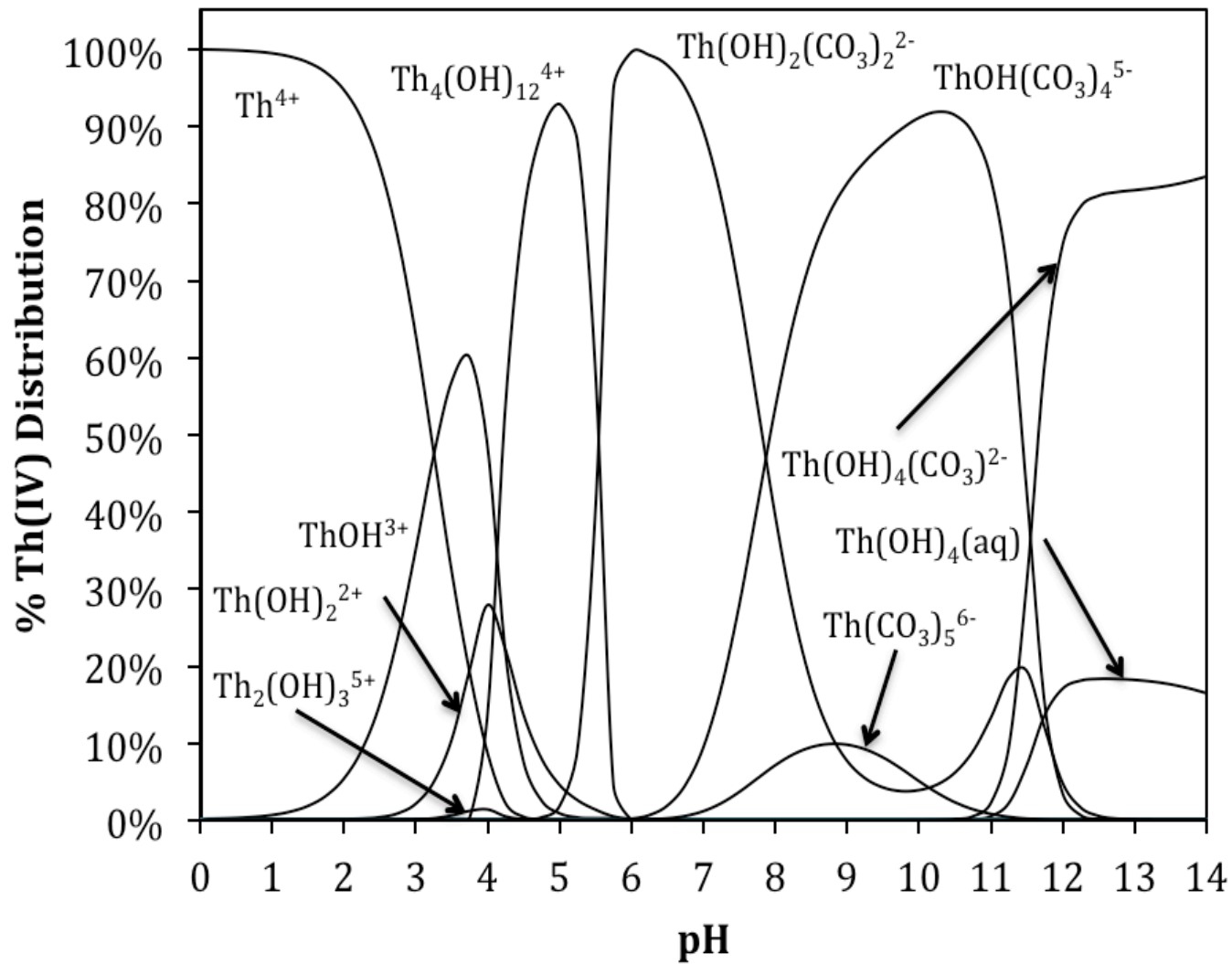


Figure 3.3: Th(IV) speciation diagram calculated using Visual MINTEQ. $C_{\text{Th}} = 3.35 \times 10^{-5} \text{ M}$, $I = 0.1 \text{ M NaHCO}_3$.

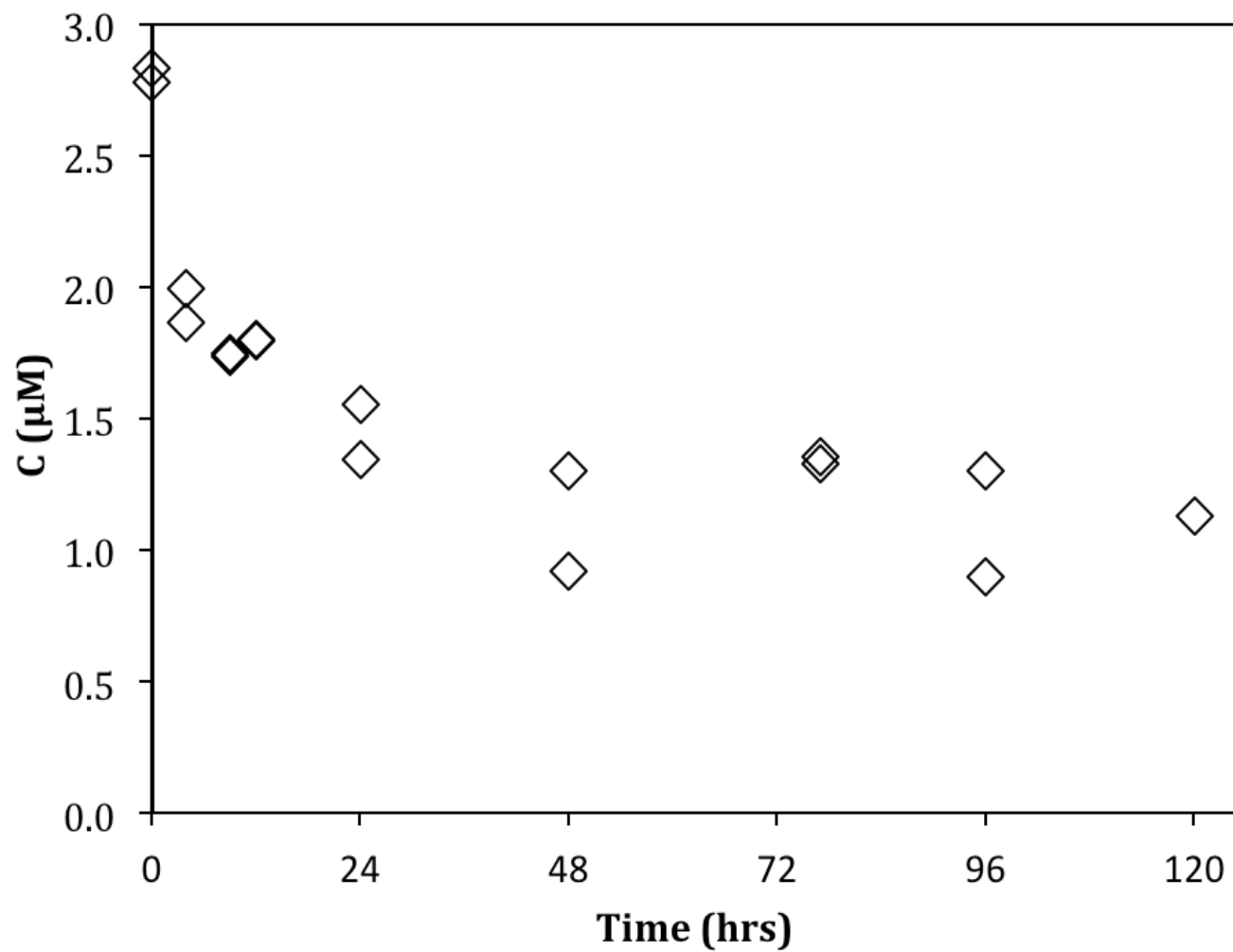


Figure 3.4: Equilibrium kinetics of Th(IV) with SRSS at $m/V = 3.33$ g/L, $C_0 = 3.08 \times 10^{-5}$ M, $I = 0.10$ M NaNO_3 , $\text{pH} = 4.15 \pm 0.09$, $\text{Temp} = 26 \pm 1$ °C.

Figure 3.4. Therefore, samples in all experiments were allowed to equilibrate for 48 hours. Control samples containing no soil (soil blanks) and samples containing no Th(IV) (Th blanks) were also made for this experiment and all other experiments using the same procedures stated above. Analysis of the soil blanks showed that there was a minor loss (<5%) due to adsorption to the tube walls, and no Th(IV) was detected in the Th(IV) blanks.

Th(IV) Isotherm

Figure 3.5 shows an adsorption isotherm of Th(IV) on SRSS soil. The isotherm is approximately linear ($r^2=0.895$) until the aqueous Th(IV) concentration exceeds the solubility of $\text{ThO}_2(\text{am, aged})$, whereby the isotherm curves sharply concave upwards, which is indicative of precipitation.

Th(IV) Precipitation

Since there is the possibility of precipitation occurring, it is necessary to determine the extent of precipitation at the Th concentrations used in experiments. Figure 3.6 shows the percent Th(IV) dissolved in solution as a function of pH in the absence of any geomedia along with the results on the basis of the theoretical solubility of $\text{ThO}_2(\text{am, fresh})$ and $\text{ThO}_2(\text{am, aged})$. Since no geomedia is present in solution, the only possible processes for Th(IV) to be removed from solution is by precipitation or adsorption to the container walls. It was noted previously that adsorption to the container walls was considered to be minor (<5%). These same results are plotted as log concentration versus pH diagram in Figure 3.7. The experimental data falls along the theoretical solubility edge of $\text{ThO}_2(\text{am, aged})$ for

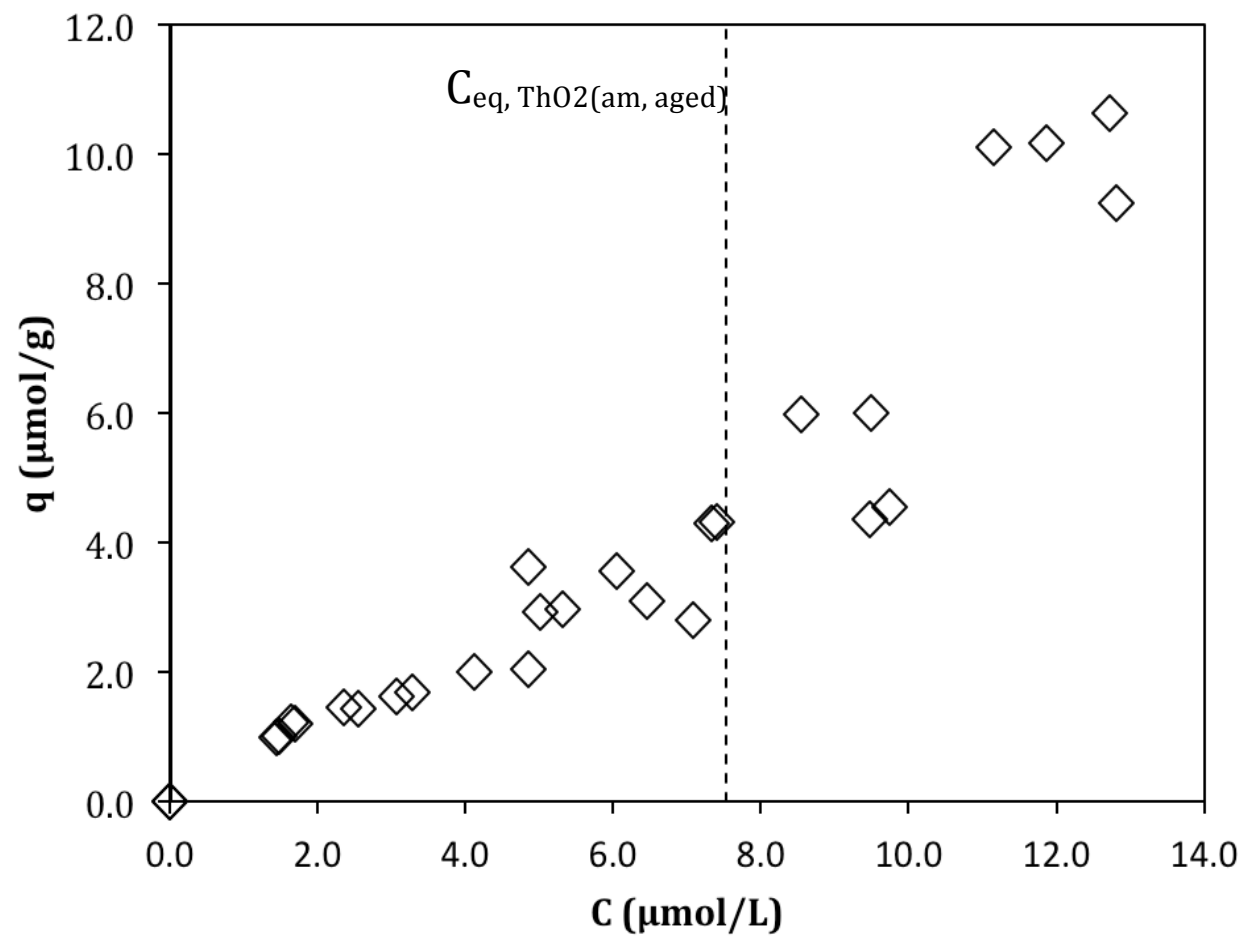


Figure 3.5: Adsorption Isotherm of Th(IV) onto SRSS; $I=0.10 \text{ M NaNO}_3$, $\text{pH}=4.13\pm 0.04$, $\text{Temp}=26\pm 1 \text{ }^\circ\text{C}$.

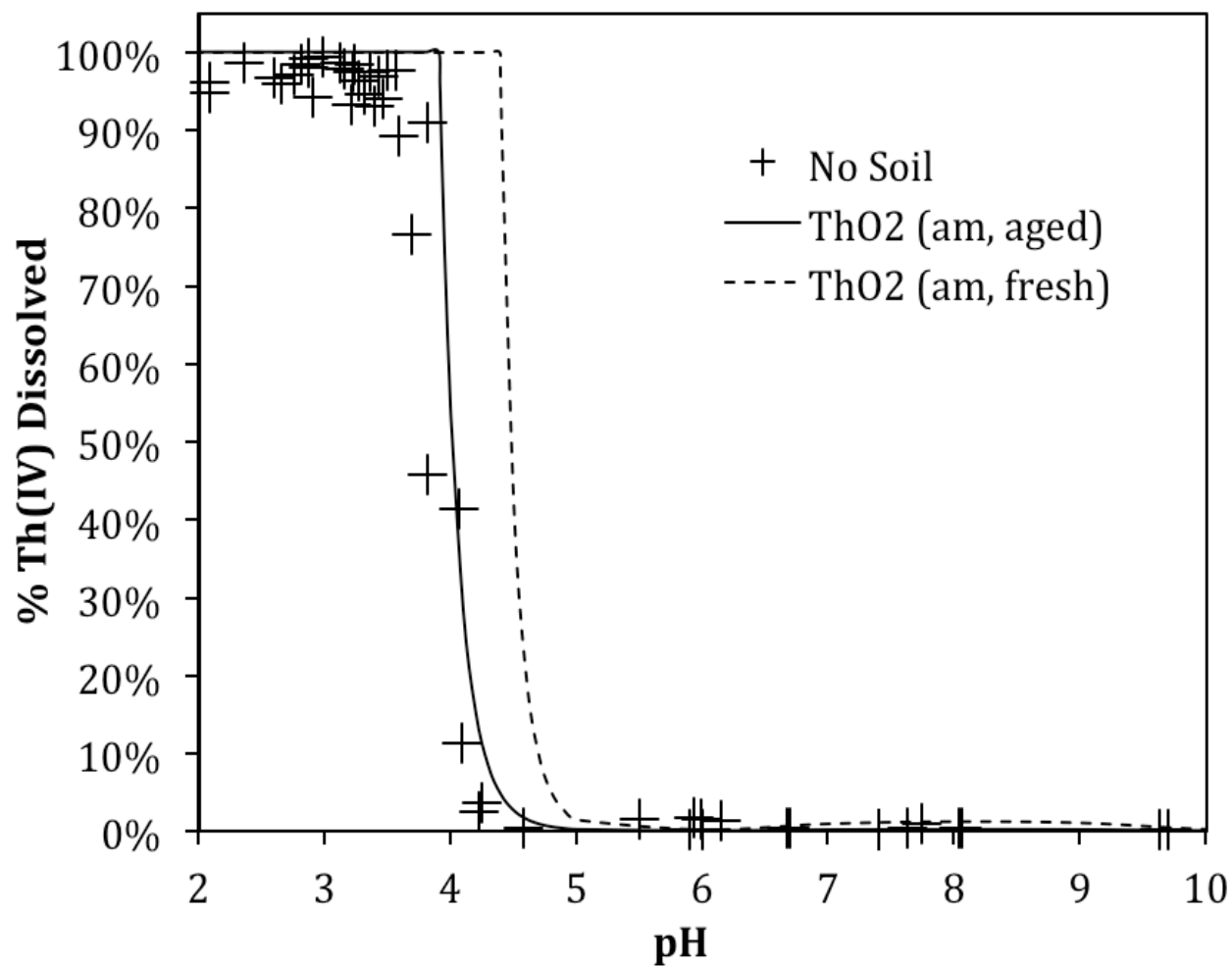


Figure 3.6: % Th(IV) Dissolved vs. pH for samples containing no soil compared to the theoretical solubility curves of ThO₂(am, fresh) ThO₂(am, aged). C₀(Th(IV)) = 3.31 x 10⁻⁵ M, I=0.09 M NaNO₃/0.01 M NaHCO₃, Temp=26±1°C

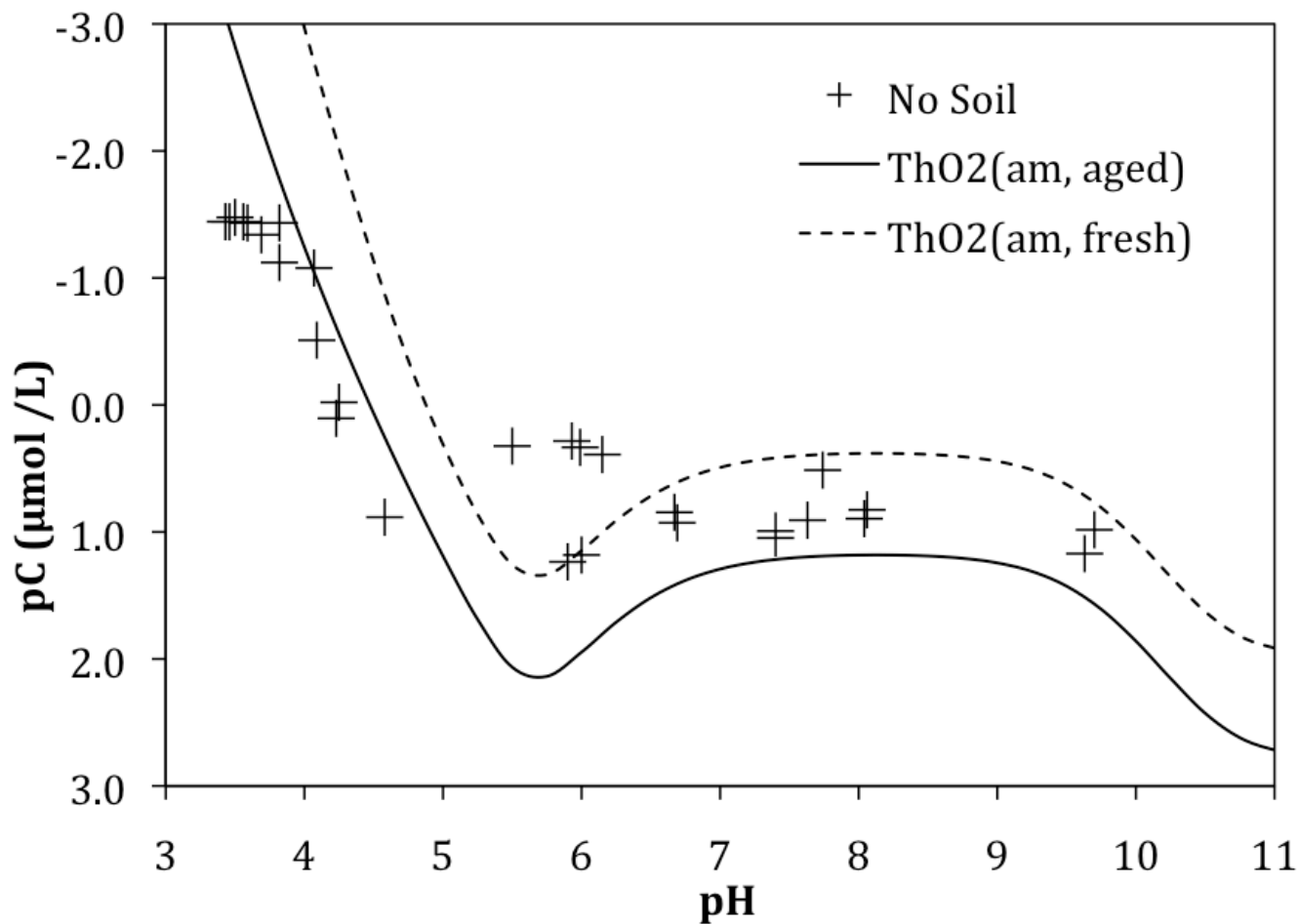


Figure 3.7: Dissolved Th(IV) concentrations vs. pH for $C_{\text{TCO}_3}=0.01$ M compared to the theoretical solubility for ThO_2 (am, fresh) and ThO_2 (am, aged), which were calculated using Visual MINTEQ and values from (Rand, Fuger et al. 2008); $C_0=3.31 \times 10^{-5}$ M; $I=0.09$ M $\text{NaNO}_3/0.01$ M NaHCO_3 , $T=26 \pm 1$ °C

pH<5, but exceeds this edge at higher pH values. This indicates that ThO₂(am, aged) is the solubility-limiting phase under acidic conditions, whereas ThO₂(am, fresh) appears to be the solubility-limiting phase under neutral and alkaline conditions. Rand, Fuger et al. (2008) suggest the solubility constant for ThO₂(am, aged) should be applied for equilibration times >70 days. However, there are instances in the literature where the solubility values for ThO₂(am, fresh) and ThO₂(am, aged) overlap (Felmy, Rai et al. 1991; Rai, Felmy et al. 1997).

In addition, the size of Th(IV) particles forming was investigated to determine if the precipitates could be considered colloids. According to the International Union for Pure and Applied Chemistry (IUPAC 2002), colloidal size is defined as particles dispersed in a medium that have at least one dimension roughly between 1 nm and 1 μm. In natural systems these colloidal particles and Th(IV) ions can accumulate on the surface of soil colloidal particles forming “pseudo-colloids.” These pseudo-colloids can enhance the mobility of Th(IV) particles since they have the ability to pass the interstitial space between larger soil particles (Cromieres, Moulin et al. 1998). In Figure 3.8, dissolved Th(IV) concentration is plotted against Th(IV) particle size removed. The solid phase was separated from the liquid phase by centrifugation in the absence of geomedia. The absence of geomedia removes the possibility of Th(IV) adsorbing to anything other than the container walls, which was noted previously to contribute <5% of Th(IV) removal. Therefore, the only other means by which Th(IV) can be removed from solution is by precipitation. In order to determine the size of Th(IV) particle removed, each sample was centrifuged

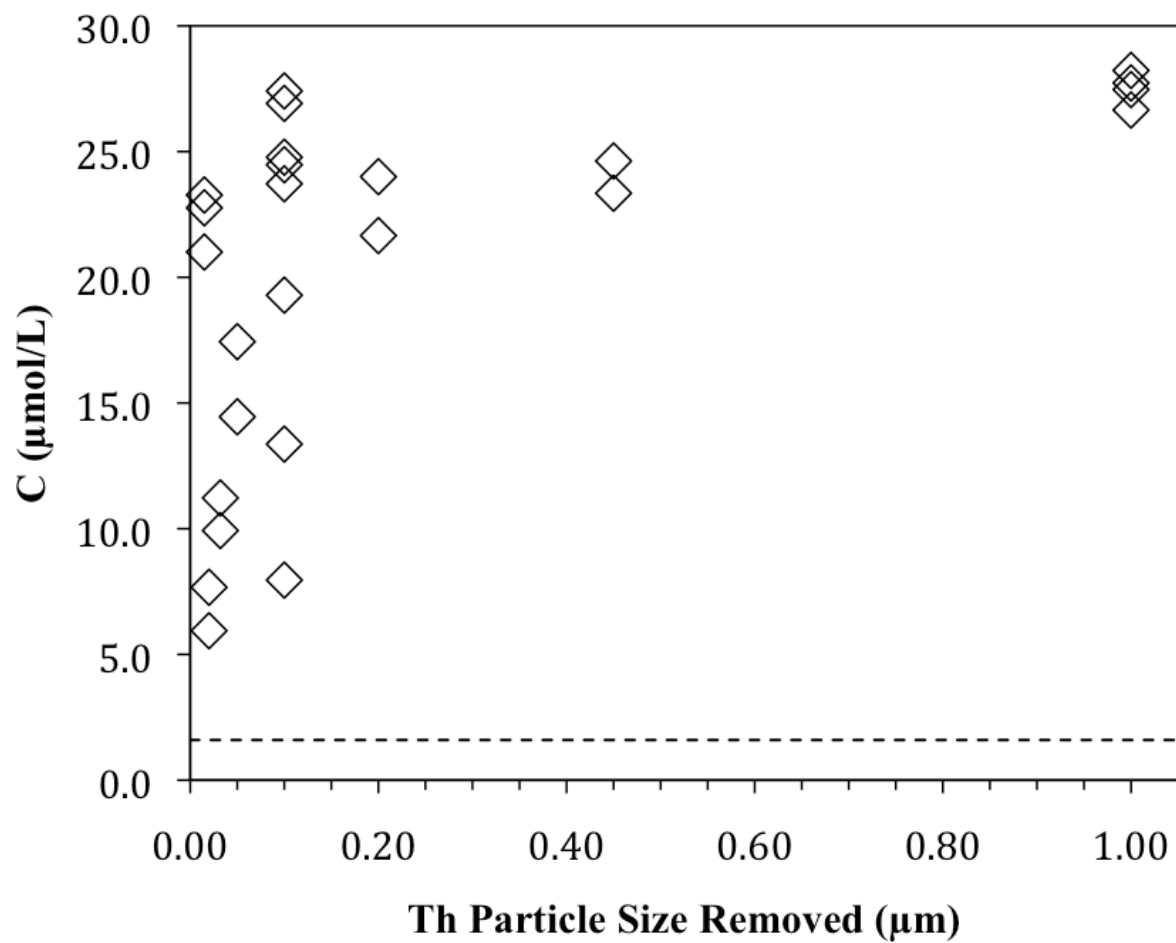


Figure 3.8: Th(IV) concentration as a function of Th(IV) particle size removed from solution by centrifugation. $\text{pH}=4.34\pm 0.08$, $C_0=3.40 \times 10^{-5}$ M, $I=0.1$ M NaNO_3 , $\text{Temp.}=26\pm 1$ °C. Dotted line shows the solubility threshold of ThO_2 (am, aged).

at distinct speeds and amounts of time as calculated by Stoke's Law (see example calculations in Appendix A) between $1\mu\text{m}$ and $0.015\mu\text{m}$. Initial ICP analysis of the samples indicated a clear drop in dissolved Th(IV) concentration. However, after performing additional trials of the experiment to reproduce the initial findings, the results became scattered as shown in Figure 3.8. The expected results were to show that as the size of the Th(IV) particle removed decreased, aqueous Th(IV) concentration also decreased. The data points in Figure 3.8 at high aqueous Th(IV) concentration and low Th(IV) particle size removed were attributed to experimenter error that was likely caused by accidental shaking of the sample when removing the sample from the centrifuge. This error may have been removed had the additional step of filtration been introduced into the experimental procedure. Although Figure 3.8 doesn't show a clear trend relating aqueous Th(IV) concentration to the size of Th(IV) particle removed, aqueous Th(IV) concentration did decrease as the Th(IV) particle size changed $1.0\mu\text{m}$ to $0.015\mu\text{m}$. These results indicate the formation of Th(IV) colloids in solution.

Formation Th(IV) Pseudo-colloids

Since Figure 3.8 indicates the formation of Th(IV) colloids in solution, the formation of pseudo-colloids was examined by redoing the Th(IV) colloid experiment with geomedia present in solution. Since geomedia is present in solution, dissolved Th(IV) can be removed by precipitation, including surface precipitation onto the geomedia, and adsorption. Pseudo-colloids may be formed by

the adsorption of radionuclides or accumulation of precipitates onto the surfaces of colloidal geomeedia.

Changes in dissolved Th(IV) concentration was analyzed with respect to the soil particle size removed by centrifugation. The resulting data in Figure 3.9 shows what appears to be a distinct decrease in dissolved Th(IV) concentrations for the range of SRSS particle sizes examined. A statistical t-test of the data determined that the aqueous Th(IV) concentrations in samples where only soil particles above 1.0 μm in size were removed are significantly ($p < 0.05$) higher than those samples where soil particles less than 0.52 μm in size were removed. This decrease in aqueous Th(IV) concentration is to be expected as smaller particles have a larger surface area relative to their volume than larger particles. The larger relative surface area provides a higher amount of adsorption sites; therefore, causing a decrease in aqueous Th(IV) concentration. Adsorption is shown to occur in Figure 3.9 in view of the fact that aqueous Th(IV) concentrations in Figure 3.9, which can be decreased by adsorption and precipitation, are generally lower, with the exception those at the lowest particle size removed, than corresponding concentrations in Figure 3.8, which were decreased only by precipitation. Furthermore, since there is drop in aqueous Th(IV) concentration in the range of colloidal, which is between 1 nm and 1 μm , Figure 3.9 indicates the formation of pseudo-colloids.

Additional t-tests revealed that there was not a significant difference between aqueous Th(IV) concentrations for samples where soil particle sizes removed from solution ranged from 0.52 μm to 0.052 μm . This test shows that the centrifugation time of 30 minutes and speed of 8000 rpm, which removed soil

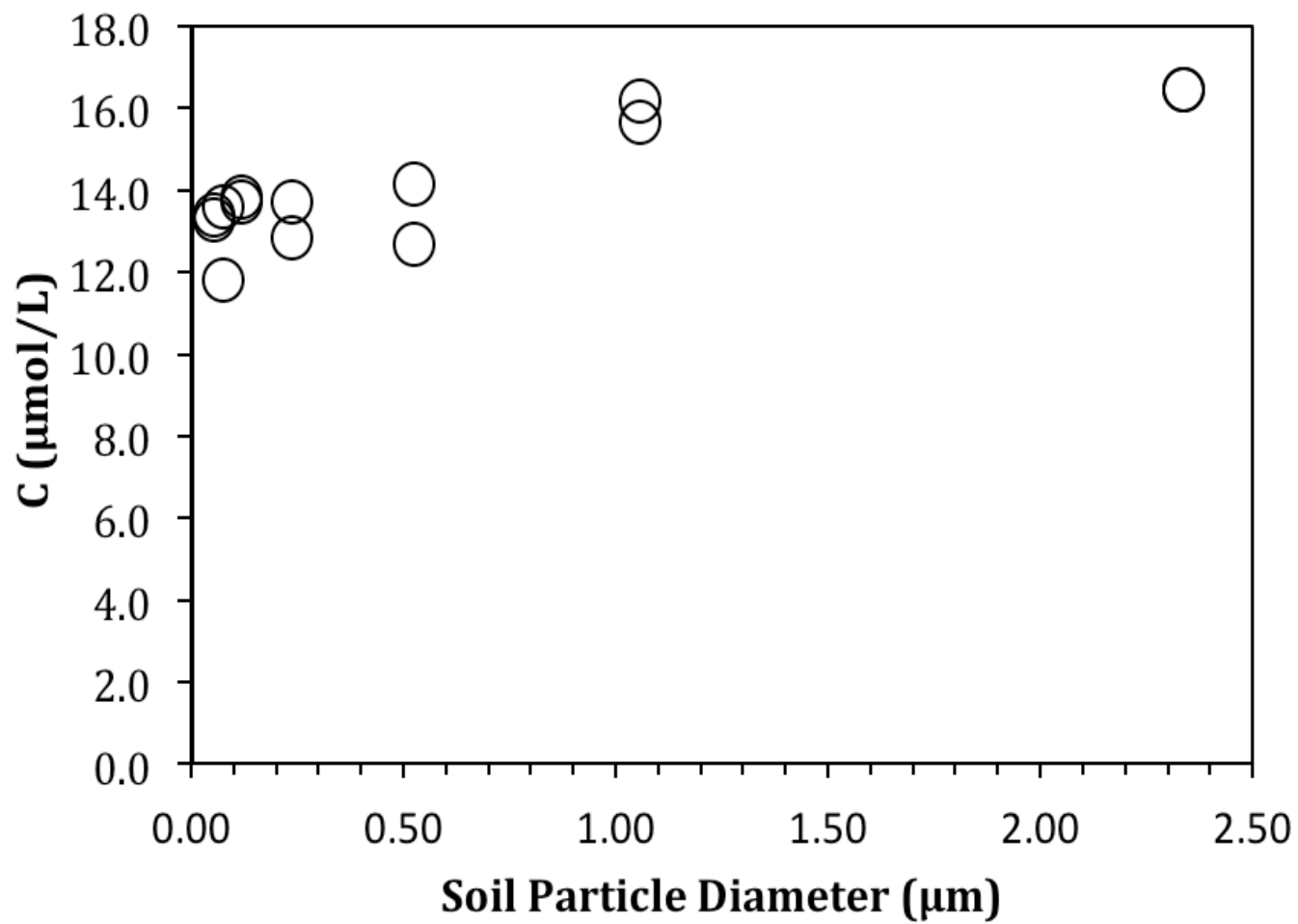


Figure 3.9: Th(IV) concentration vs. SRSS particle size at $m/V=3.31$, $C_0=3.05 \times 10^{-5}$, $I=0.1$ M NaNO_3 , $\text{pH}=4.19 \pm 0.04$, $\text{Temp}=26 \pm 1^\circ\text{C}$.

particles 0.074 μm in size, used in the experimental methods effectively removed a maximum amount of Th(IV) particles from solution.

Th(IV) Sorption onto SRSS

The sorption of Th(IV) onto SRSS is shown in Figure 3.10 plotting percent dissolved as a function pH. When plotting adsorption as a function of pH, percent adsorbed (or dissolved) is less sensitive than plotting $\log K_D$ or q as a function of pH, which can vary by several orders of magnitude (Hartzog, Loganathan et al. 2009). Also, the experimental data would not be able to be compared to the theoretical solubility curves of $\text{ThO}_2(\text{am, fresh})$ and $\text{ThO}_2(\text{am, aged})$ if the data were plotted as $\log K_D$ or q vs. pH. Thorium sorption with a total carbonate concentration (C_{TCO_3}) of 0.01 M was studied in the pH range of 2-10 with a Th(IV) concentration of 3.34×10^{-5} M and SRSS solid-solution ratios (m/V) of 0.51 g/L to 31.62 g/L with an ionic strength $I=0.09$ M $\text{NaNO}_3/0.01$ M NaHCO_3 . Th(IV) sorption is shown to be strongly dependent on pH with the sorption edge observed at $\text{pH} \approx 3.5$. At the m/Vs 0.51 g/L and 2.68 g/L the Th(IV) concentration values fall along the $\text{ThO}_2(\text{am, aged})$ solubility edge, which is similar to Th(IV) concentration values in the absence of geomeedia in Figure 3.6. This indicates that precipitation is the major removal mechanism at these m/Vs. Once the SRSS m/V was increased by a factor of ten to 31.62 g/L, adsorption began to play a noticeable role in dissolved Th(IV) removal.

Th(IV) Sorption onto SRSC

The sorption of Th(IV) onto SRSC was tested under the same experimental conditions as SRSS, and the results are shown in Figure 3.11. The sorption edges for

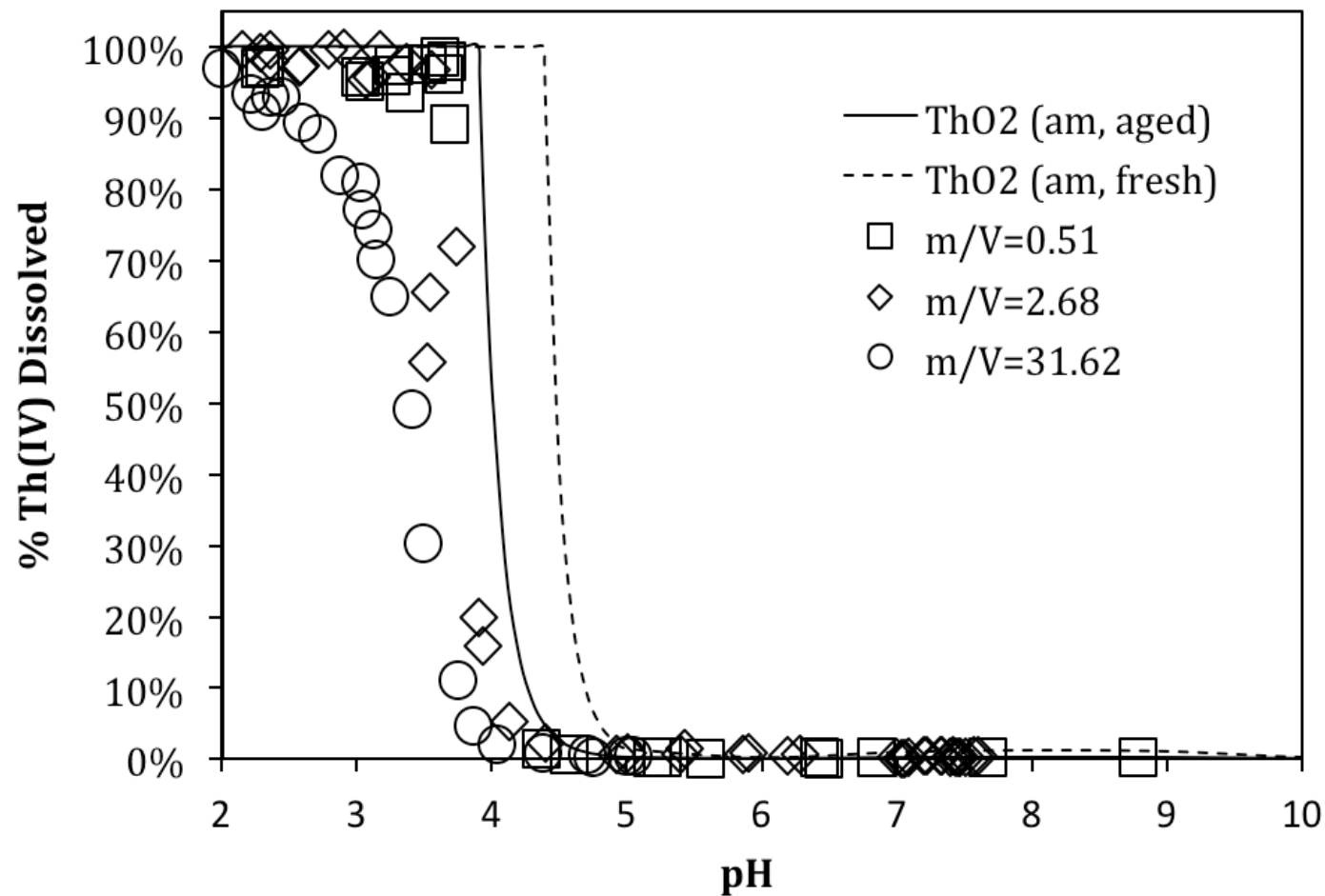


Figure 3.10: % Th(IV) Dissolved vs. pH for different m/Vs of SRSS. $C_0(\text{Th(IV)}) = 3.34 \times 10^{-5} \text{ M}$, $I=0.09 \text{ M NaNO}_3/0.01 \text{ M NaHCO}_3$, $\text{Temp}=26\pm 1^\circ\text{C}$

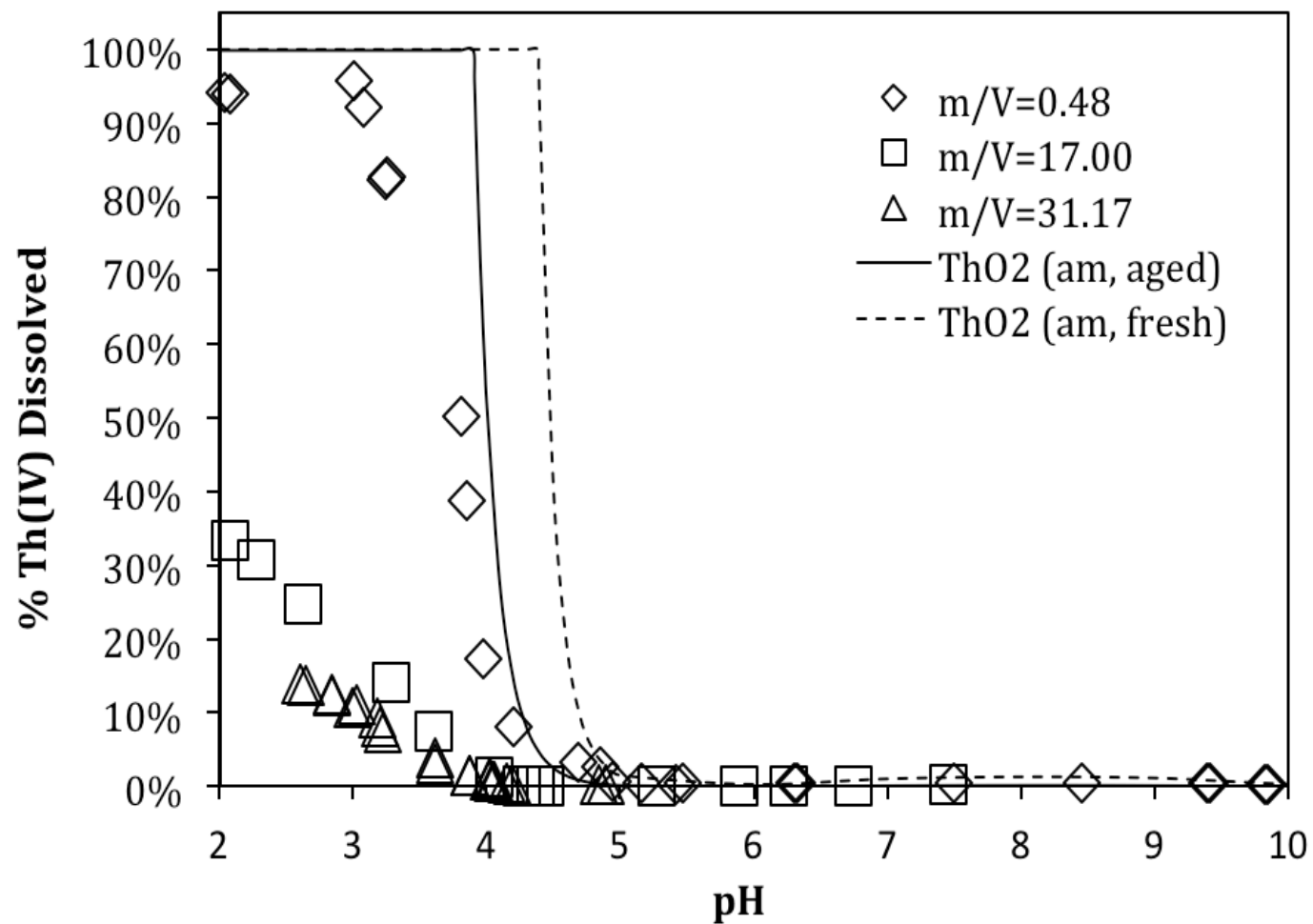


Figure 3.11: % Th(IV) Dissolved vs. pH for different m/Vs of SRSC. $C_0(\text{Th(IV)}) = 3.30 \times 10^{-5} \text{ M}$, $I=0.09 \text{ M NaNO}_3/0.01 \text{ M NaHCO}_3$, $\text{Temp}=26\pm 1^\circ\text{C}$

the m/Vs of 0.48 g/L for SRSC and 0.51 g/L for SRSS are similar, indicating that precipitation is controlling dissolved Th(IV) removal here as well. It is observed that adsorption begins to play a greater role at about half the m/V for SRSC (17.00 g/L) than SRSS (31.62 g/L). At pH=3 the % Th(IV) dissolved in samples containing SRSS is approximately 80% for a m/V of 31.17. Whereas, at a similar m/V and pH value, the % Th(IV) dissolved in samples containing SRSC is approximately 10%. Powell, Fjeld et al. (2002) achieved similar results for the sorption of Pu(IV) on SRS soils with comparable characteristics. It was also shown that after 33 days, the sorption edge for the subsurface soils used in that study for Pu(V) was similar to the sorption edge for Pu(IV) at 0 days, which indicates that Pu(V) is being reduced to Pu(IV) in those systems (Powell, Fjeld et al. 2002). Since the SRS soils in this study have comparable characteristics, it is likely that they would also produce a reducing environment as well, which would make it possible sorbent for redox sensitive actinides such as U, Np, or Pu.

The increased adsorption of SRSC is probably due to a larger BET surface area, higher cation exchange capacity (CEC), and higher percentage of organic matter (OM) (15.31 m²/g, 1.09 cmol/kg, and 8.8%, respectively) than SRSS (1.27 m²/g, -0.35 cmol/kg, and 0%, respectively). These soil characteristics are important because they can have a large effect on the sorption of positively metal ions such as Th(IV), which is shown when comparing Figure 3.10 to Figure 3.11. If a soil has a higher surface area, it contains more surface sites to which contaminants can adsorb. CEC refers to the quantity of cations that a soil can adsorb or exchange. Generally, CEC is dependent on the surface area and amount of organic matter

contained in a soil. Therefore, a soil with higher clay and organic matter content tends to have a higher CEC because these soils contain a high ratio of small particles and have a negative surface charge.

Th(IV) Sorption onto Goethite

The sorption of Th(IV) onto synthetic goethite is shown in Figure 3.12. The sorption edge for goethite is observed at $\text{pH} \approx 3.0$ for a m/V of 15.81. Like SRSS and SRSC, the primary mechanism for dissolved Th(IV) removal in this system at m/V 0.49 g/L is precipitation. It is observed in Figure 3.12 that like SRSC adsorption begins to participate a noticeable role at a low m/V of 3.28 g/L for goethite. However, the sorption edge for goethite is sharper than SRSC. At $\text{pH}=3$, sorption is at approximately 90% for goethite m/V of 15.81 g/L and about 80% for SRSC m/V of 17.00 g/L. Whereas, sorption at $\text{pH}=2$ is about 85% and 35% for the same m/V for goethite and SRSC, respectively. Rojo, Seco et al. (2009) used similar experimental conditions with an m/V of 10 g/L magnetite or ferrihydrite and a total Th(IV) concentration of 1.1×10^{-6} M. They achieved similar sorption edges with 50% Th(IV) sorption at $\text{pH} \sim 2.2$ and 2.9 in their study of Th(IV) sorption onto magnetite and ferrihydrite, respectively. Laflamme and Murray (1987) studied the adsorption of Th(IV) onto goethite and their sorption edge was most comparable to the m/V=15.81 g/L. However, their study was conducted at low Th(IV) concentrations of 10^{-13} M and a low goethite m/V of 5.22 mg/L. These results show that goethite will strongly inhibit the mobility of Th(IV) in natural subsurface water systems.

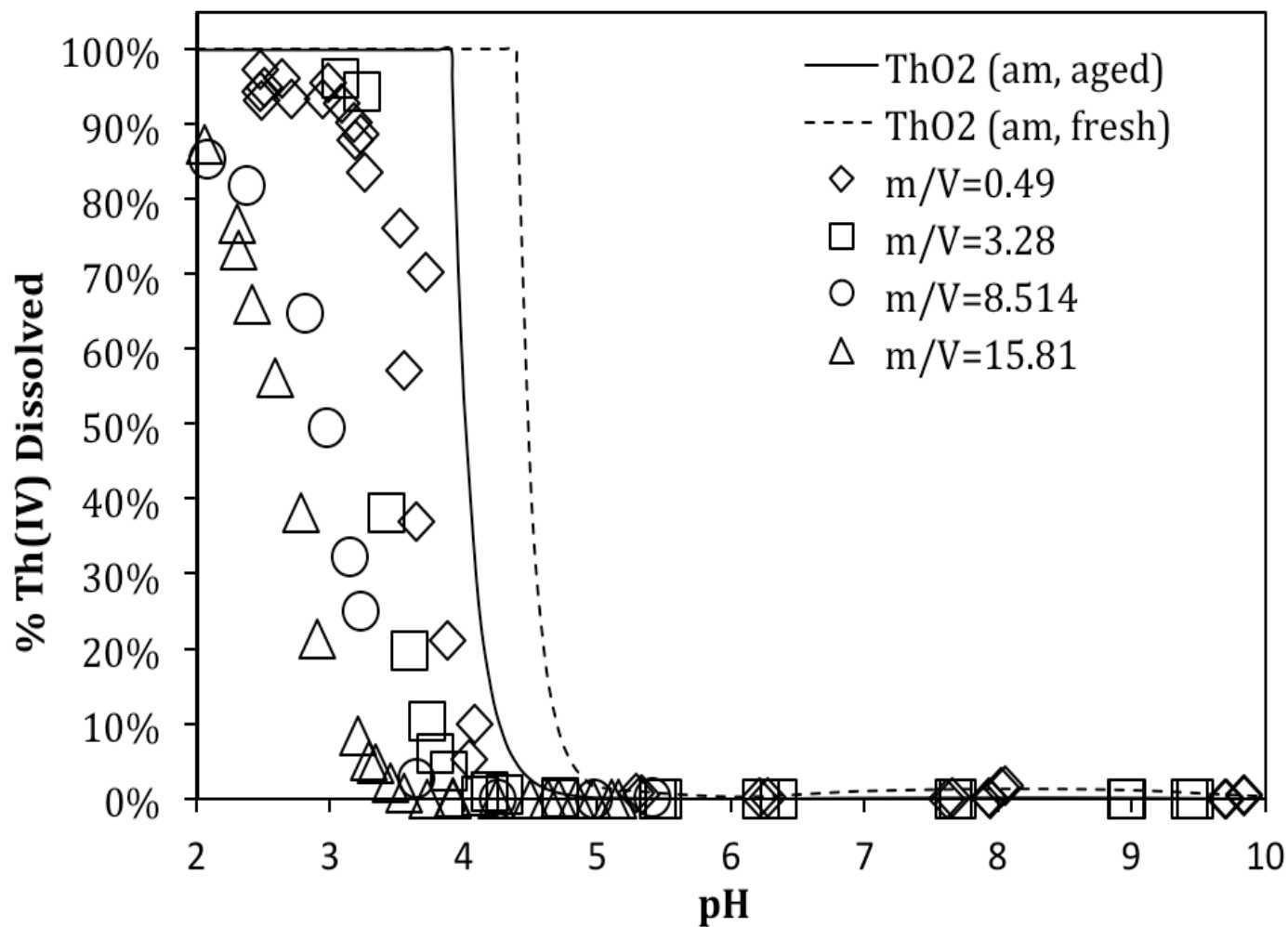


Figure 3.12: % Th(IV) Dissolved vs. pH for different solid-solution ratios of goethite. $C_0(\text{Th(IV)}) = 3.34 \times 10^{-5} \text{ M}$, $I=0.09 \text{ M NaNO}_3/0.01 \text{ M NaHCO}_3$, $\text{Temp}=26\pm 1^\circ\text{C}$

Th(IV) Sorption onto Kaolinite

The sorption of Th(IV) onto kaolinite is shown in Figure 3.13. A pH range of 2-12 was investigated instead a pH of 2-10 for the other soils because of the increase in dissolved Th(IV) at high pH values. Adsorption of Th(IV) onto kaolinite is the dominant removal mechanism at a pH<4 in this system even with a low solid-solution ratio. However, as pH becomes more neutral and alkaline, Th(IV) becomes oversaturated with respect ThO₂ (am, fresh) and ThO₂ (am, aged), and the oversaturation increases with an increase in m/V. Since kaolinite has a negatively charged surface and at pH>5 negatively charged Th-hydroxo-carbonate species predominate, it is expected that sorption would decrease somewhat in this pH range. According to Banik, Buda et al. (2007), kaolinite is found to be slightly soluble in the near neutral pH range 5-8 with solubility increasing at pH>8. This may help explain the cause for the increase in dissolved Th(IV) concentrations above at pH>8. In their study of Pu(IV) sorption onto kaolinite in the presence of carbonate, Banik, Buda et al. (2007) found that Pu(IV) and Th(IV) sorption decreased at pH>8.5 similar to the decrease shown in Figure 3.13. Banik, Buda et al. (2007) attributed this decrease to the formation of negatively charged Th-hydroxo-carbonate species. This conclusion may have some merit as the ternary carbonate species Th(OH)₂(CO₃)₂²⁻ becomes the dominant species from pH ~6.5 to 10.5 as shown in Figure 3.2. However, if this species affected Th(IV) sorption to such a degree it would have also affected Th(IV) sorption onto other geomedia discussed above. Th(IV) concentrations from pH 6 to 11 are about 2 orders of magnitude greater than

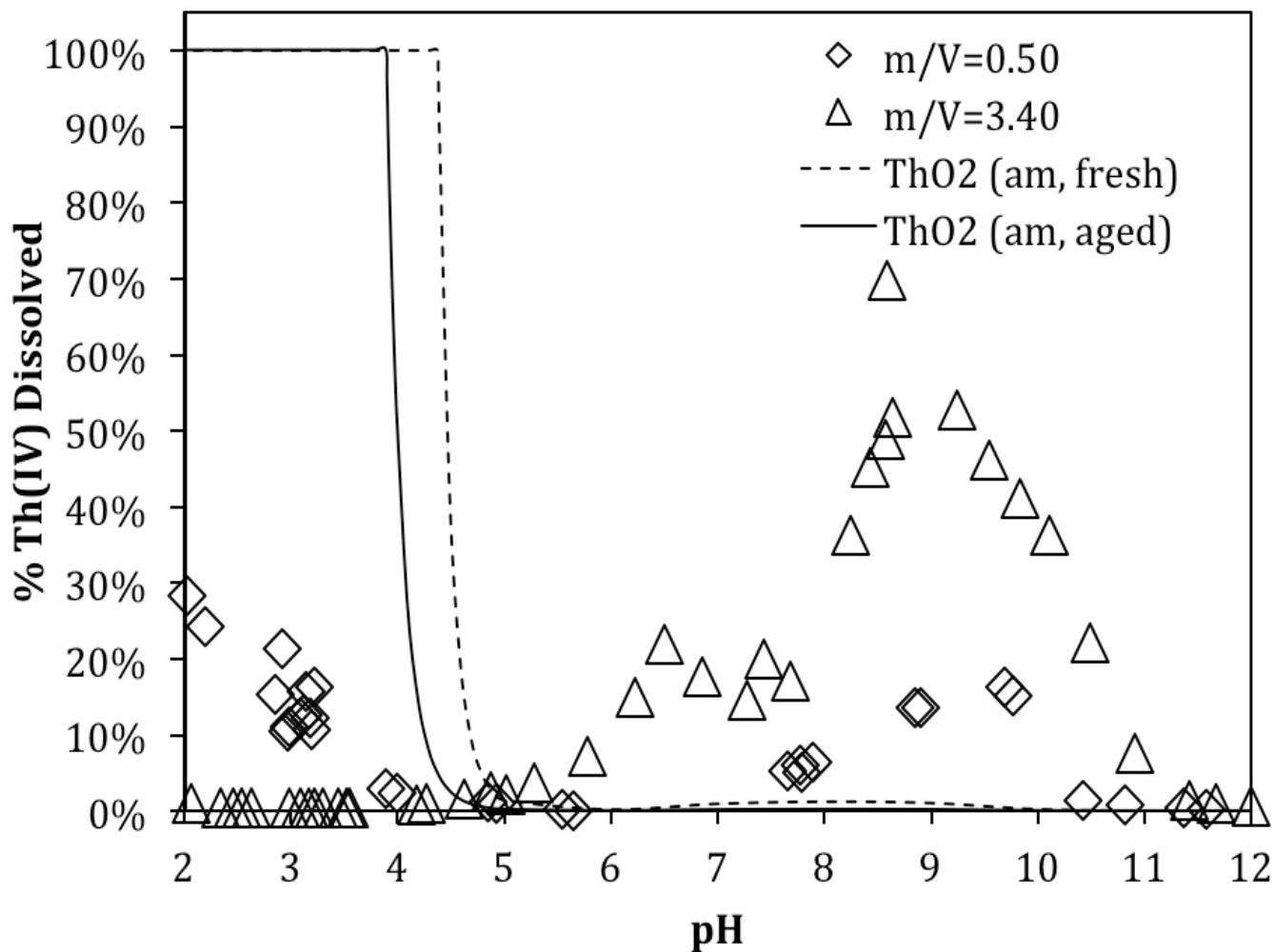


Figure 3.13: % Th(IV) Dissolved vs. pH for different m/Vs of kaolinite. $C_0(\text{Th(IV)}) = 3.34 \times 10^{-5}$ mol/L, $I=0.09$ M $\text{NaNO}_3/0.01$ M NaHCO_3 , $\text{Temp}=26\pm 1^\circ\text{C}$

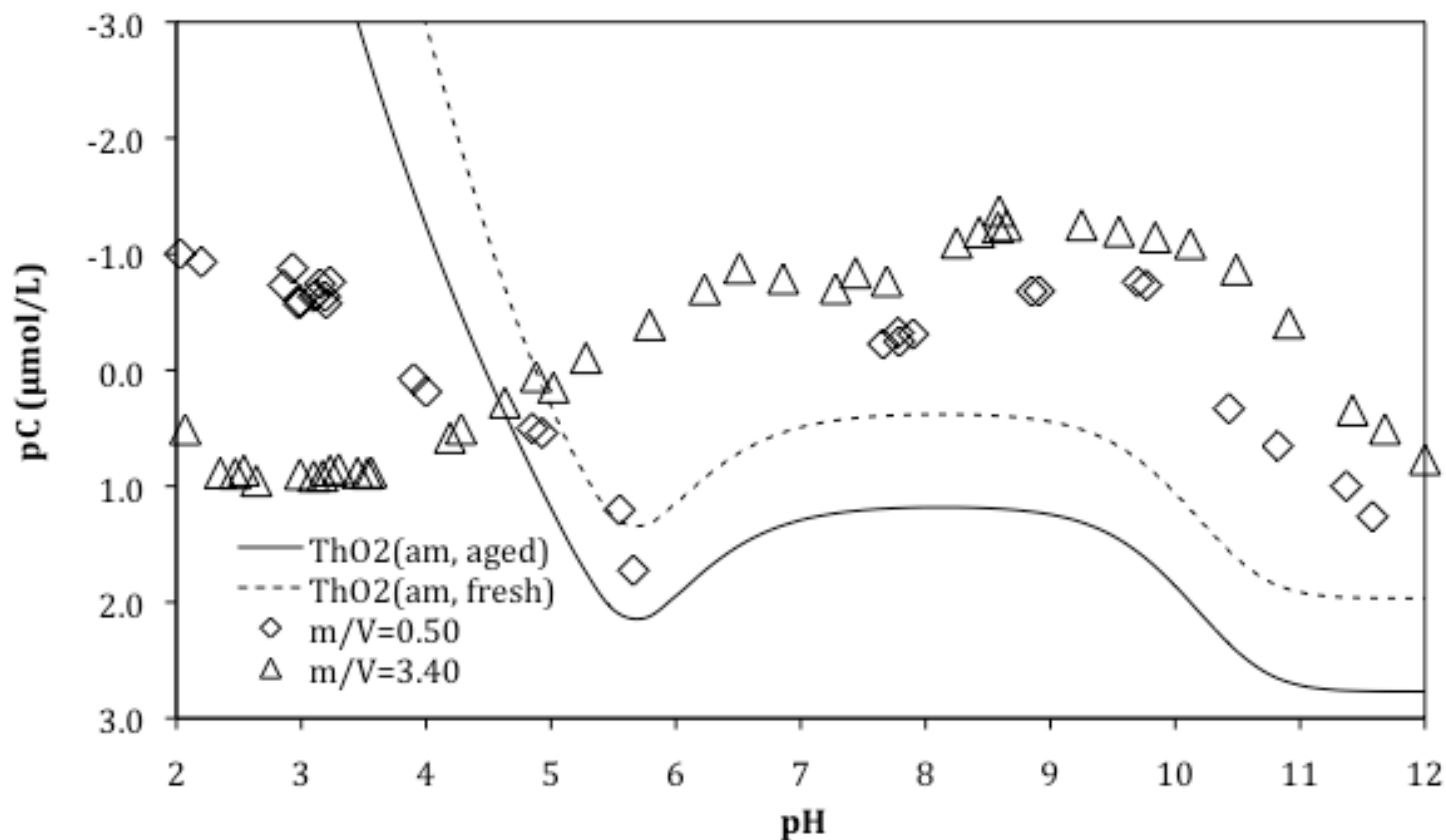


Figure 3.14: Dissolved Th(IV) concentrations vs. pH for for different m/Vs of kaolinite compared to the theoretical solubility for ThO₂ (am, fresh) and ThO₂ (am, aged), which were calculated using Visual MINTEQ and values from (Rand, Fuger et al. 2008); $C_0=3.34 \times 10^{-5}$ M; $I=0.09$ M NaNO₃/0.01 M NaHCO₃, $T=26\pm 1$ °C

the solubility of ThO₂(am, aged) (shown in Figure 3.14) while Th(IV) concentrations in samples containing other geomeia were below saturation.

Effect of Carbonate on Th(IV) Sorption

The effect of carbonate concentration on Th(IV) sorption onto SRSS and SRSC was also investigated. Initial experiments were conducted to test whether precipitation is still occurring at $C_{\text{TCO}_3} = 0.1$ M. Figure 3.15 plots the dissolved Th(IV) concentration against pH (2-12) in the absence of geomeia and indicates that precipitation still occurs. Th(IV) is shown to be supersaturated with respect to ThO₂(am, fresh) at $\text{pH} \approx 11$. These results are also plotted on as log solubility versus pH in Figure 3.16. When compared to the sorption of Th(IV) onto SRSS and SRSC at lower carbonate concentrations, the increase in solubility in the pH range 5-11 is likely due to increased concentrations of Th-hydroxo-carbonate complexes, which are the dominant species in this range as shown in Figure 3.3. Altmaier, Neck et al. (2005) attributes the increase in solubility specifically to the highly negative Th-hydroxo-carbonate species $\text{ThOH}(\text{CO}_3)_4^{-5}$ and $\text{Th}(\text{CO}_3)_5^{-5}$, the former being the predominant species from pH 8 to 11.5 as shown in Figure 3.3.

Figure 3.17 shows the effect of increased carbonate concentration on the sorption of Th(IV) onto SRSS. The increase in carbonate concentration does not have much effect on Th(IV) sorption at $\text{pH} < 5$. However, it is observed that precipitation looks to be the dominating removal mechanism in this range. From pH 5 to 10, the % Th(IV) dissolved in solution increases significantly from $< 1\%$ to $\sim 80\%$ and drops back to $\sim 1\%$ at $\text{pH} \approx 12$. Adsorption does not seem to be dominating Th(IV) removal

from solution at pH<6 but is observed to have some effect at pH 6-11. Laflamme and Murray (1987) examined the effect of carbonate concentration on Th(IV) sorption onto goethite and found that adsorption dropped to effectively 0% at pH ~9 at 300 meq/L carbonate alkalinity. The results shown in Figure 3.10 and Figure 3.17 suggest that SRSS does not look to be an effective adsorbent for Th(IV) at the m/Vs used. Figure 3.18 shows the effect of increased carbonate concentration on the sorption of Th(IV) onto SRSC. Adsorption is strongly influenced by pH. Although the results for samples containing no geomeedia and SRSC concentration of 0.49 g/L are similar, it appears that adsorption is playing a role in Th(IV) removal at pH 6-10.5, even at this low m/V. At the higher m/V of 16.41 g/L, adsorption is clearly the major removal mechanism in this system. As noted previously, Th(IV) sorption onto SRSC is greater than SRSS because SRSC has a larger BET surface area, higher CEC, and higher percentage OM.

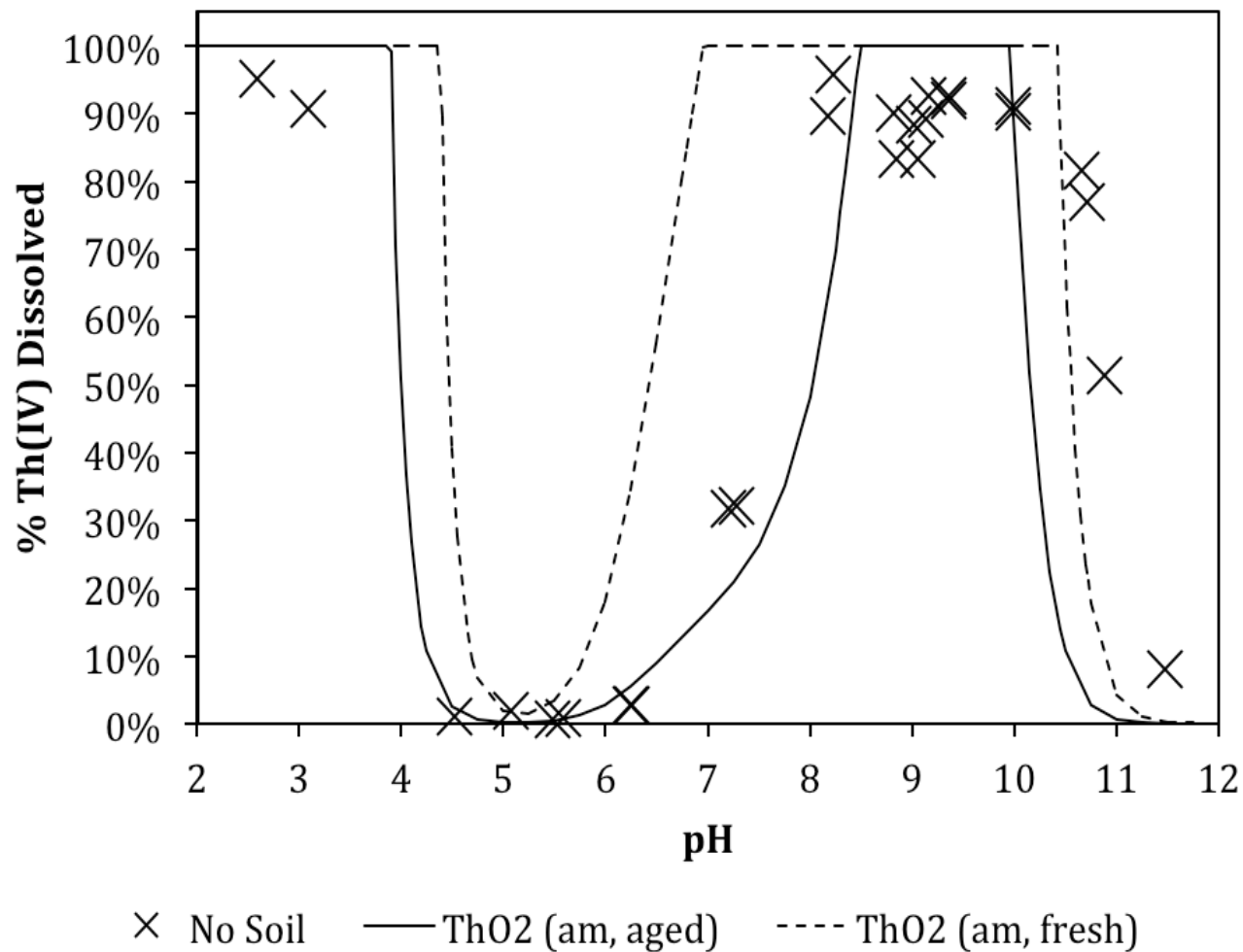


Figure 3.15: % Th(IV) Dissolved vs. pH at $C_{\text{TCO}_3}=0.1$ M; $C_0=3.40 \times 10^{-5}$ mol/L, $I=0.1$ M NaHCO₃, Temp.= 26 ± 1 °C. Results for samples containing no geomeedia are compared with theoretical solubility curves for ThO₂ (am, fresh) and ThO₂ (am, aged).

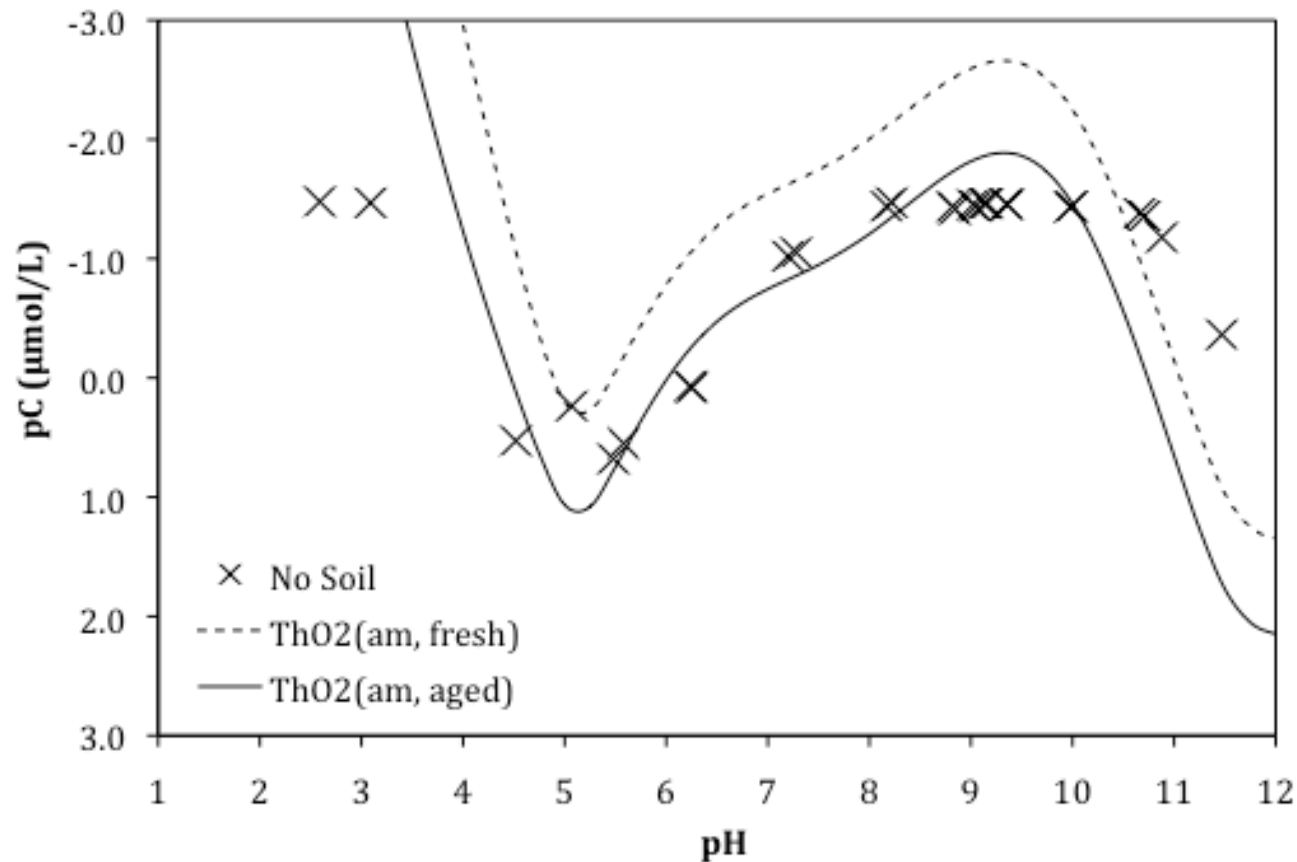


Figure 3.16: Dissolved Th(IV) concentrations vs. pH for $C_{\text{TCO}_3}=0.1$ M compared to the theoretical solubility for ThO₂ (am, fresh) and ThO₂ (am, aged), which were calculated using Visual MINTEQ; $C_0=3.34 \times 10^{-5}$ M; $I=0.1$ M NaHCO₃, $T=26 \pm 1$ °C

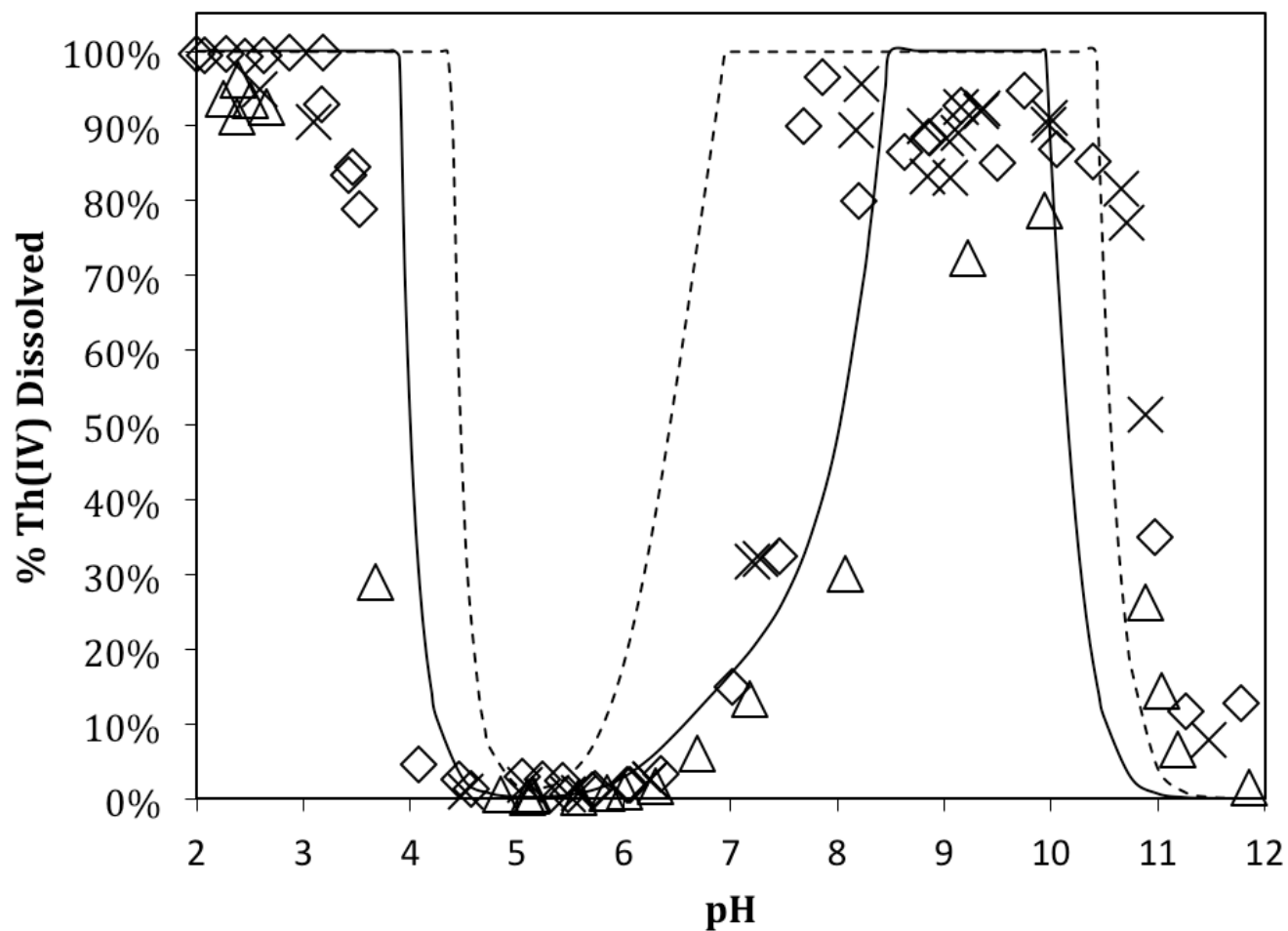


Figure 3.17: % Th(IV) Dissolved vs. pH for SRSS at $C_{\text{TCO}_3}=0.1$ M; $C_0=3.40 \times 10^{-5}$ mol/L, $I=0.1$ M NaHCO₃, Temp.= 26 ± 1 °C. Experimental results at SRSS concentrations of 0.49 g/L (◇) and 16.33 g/L (△) compared to samples containing no geomedia (×) and the theoretical solubility curves for ThO₂ (am, fresh) (dashed line) and ThO₂ (am, aged) (solid line).

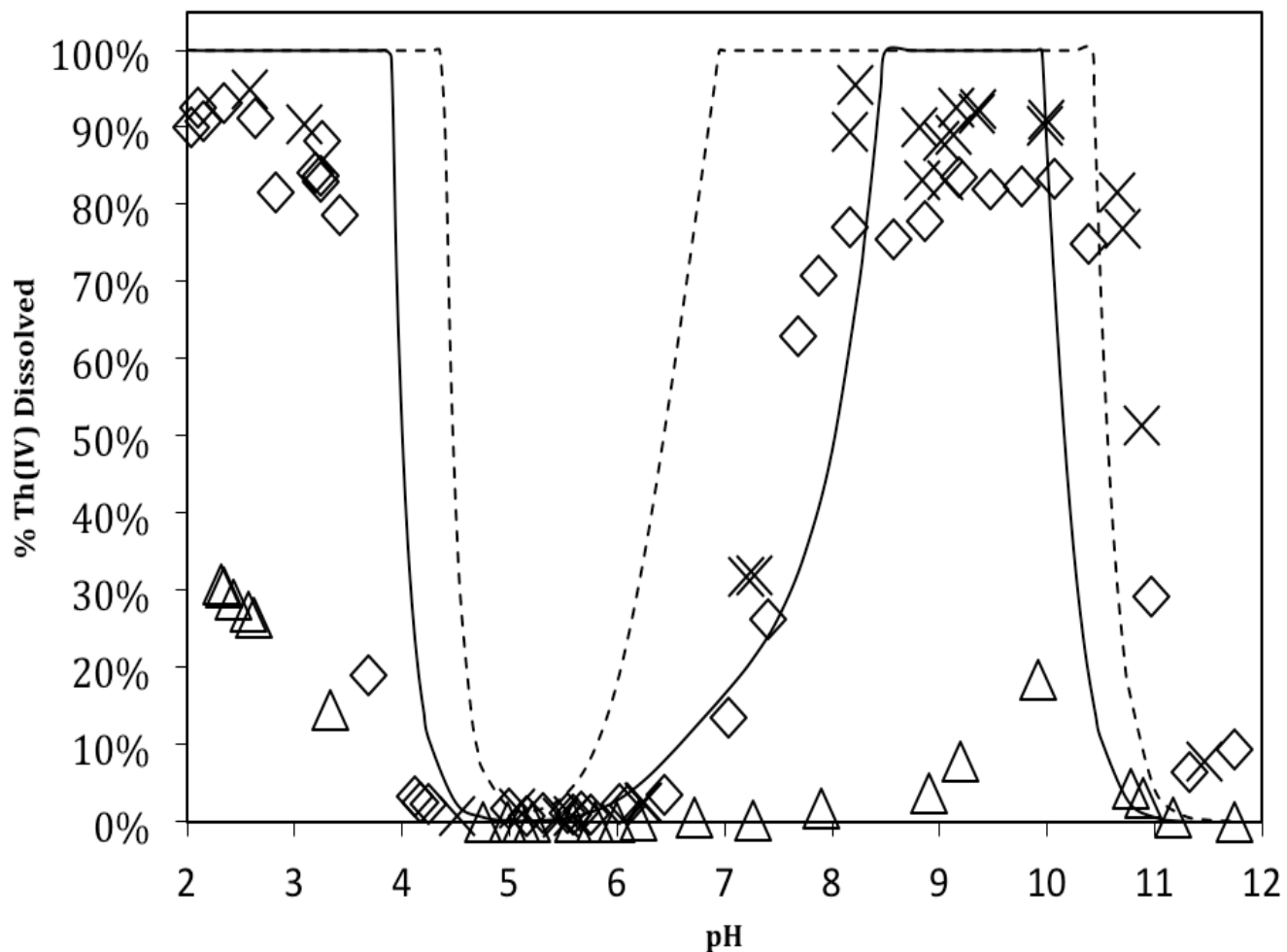


Figure 3.18: % Th(IV) Dissolved vs. pH for SRSC at $C_{\text{TCO}_3}=0.1$ M; $C_0=3.40 \times 10^{-5}$ mol/L, $I=0.1$ M NaHCO_3 , $\text{Temp.}=26\pm 1$ °C. Experimental results at SRSC concentrations of 0.49 g/L (\diamond) and 16.41 g/L (Δ) compared to samples containing no geomeedia (\times) and the theoretical solubility curves for ThO_2 (am, fresh) (dashed line) and ThO_2 (am, aged) (solid line).

Chapter 4.

Conclusions and Recommendations for Future Work

4.1 Conclusions

1. Results indicate that “true” Th(IV) colloids may form in the absence of geomedia, whereas pseudo-colloids may form in the presence of geomedia. Precipitation has been shown to be a major removal mechanism at the Th(IV) concentrations used in this study in the absence of geomedia and at low solid-solution ratios. Rand, Fuger et al. (2008) state that ThO₂(am) solubility should not be affected by aging if experiments were conducted in timeframes less than 25 days. Yet, the results show that the solubility limiting factor in this study was ThO₂(am, aged), which should only be of major concern for experimental timeframes greater than 70 days.
2. Thorium sorption was shown to be strongly dependent on pH, solid-solution ratio, and carbonate concentration.
3. In the presence of carbonate (0.01 M), sorption edge results show greater adsorption for SRSC and goethite than SRSS with adsorption percentage reaching >95% between pH 3.5 and 4. The increased adsorption results were attributed to greater specific surface area and other factors such as CEC and organic matter content.

4. At higher carbonate concentrations (0.1 M), the solubility of Th oxide solids increases approximately by two orders of magnitude from pH 5 to pH 9.5. There was also a decrease in the adsorption of Th(IV) onto SRSS and SRSC in this pH range, which corresponds to an increased concentration of negatively charged ternary Th-hydroxo-carbonate species.
5. SRS soils with similar soil characteristics to SRSS and SRSC and other iron oxides have been shown to reduce Pu(V) to Pu(IV) in sorption studies (Powell, Robert et al. 2002; Powell, Fjeld et al. 2004; 2005). This reduction would be beneficial to further inhibiting the mobility of actinides since the tetravalent state is the least mobile oxidation state (Choppin 2007).
6. Th(IV) was shown to strongly adsorb to kaolinite at pH<5, but was poorly adsorbed between pH 5 and pH 11. The decrease in adsorption in this pH range of may be partially due to the increased concentration of negatively charged ternary Th-hydroxo-carbonate species as kaolinite has a net negative surface charge. Banik, Buda et al. (2007) reached a similar conclusion in their study on Pu(IV) sorption onto kaolinite.
7. Interestingly, dissolved Th(IV) concentration increased with an increase in the kaolinite m/V in the pH range 5-11. This increase in aqueous Th(IV) concentration was about 2 orders of magnitude greater than ThO₂(am, aged), which cannot be explained by previous conclusions that negatively charged ions were a major cause in a decrease in adsorption. This increase shows that kaolinite may increase the mobility of Th(IV) in subsurface environments.

4.2 Recommendations for Future Work

1. Further experiments at a lower total Th(IV) concentration need to be conducted to see if the solubility limiting factor changes to ThO₂(am, fresh). Also, aging experiments should be conducted to observe if there are any further reductions in solubility in these systems.
2. Further adsorption analysis, such as x-ray diffraction or x-ray absorption fine structure analyses, on Th(IV) ions onto SRSS and SRSC sediment surfaces needs to be conducted to determine what surface complexes form (i.e., monodentate or bidentate).
3. Since colloids can have a significant effect on the transport of contaminants in subsurface, column studies need to be employed to see how Th(IV) reacts in a transport system.
4. Further investigation on the Th-carbonate-kaolinite system is needed to better understand what processes are occurring at pH>5 to cause a dissolved Th(IV) concentration to be two orders of magnitude greater than the solubility curve of ThO₂ (am, aged).

References

- Altmaier, M., V. Neck, M. A. Denecke, R. Yin and T. Fanghanel (2006). "Solubility of $\text{ThO}_2 \cdot x\text{H}_2\text{O}(\text{am})$ and the formation of ternary Th(IV) hydroxide-carbonate complexes in NaHCO_3 - Na_2CO_3 solutions containing 0-4 M NaCl." *Radiochimica Acta* **94**(9-11): 495-500.
- Altmaier, M., V. Neck and T. Fanghanel (2004). "Solubility and colloid formation of Th(IV) in concentrated NaCl and MgCl_2 solution." *Radiochimica Acta* **92**(9-11): 537-543.
- Altmaier, M., V. Neck, R. Muller and T. Fanghanel (2005). "Solubility of $\text{ThO}_2 \cdot x\text{H}_2\text{O}(\text{am})$ in carbonate solution and the formation of ternary Th(IV) hydroxide-carbonate complexes." *Radiochimica Acta* **93**(2): 83-92.
- ATSDR. (2009, Sept. 1, 2009). "2007 CERCLA Priority List of Hazardous Substances." *CERCLA Priority List of Hazardous Substances* Retrieved May 31, 2011, from <http://www.atsdr.cdc.gov/cercla/07list.html>.
- ATSDR. (2011, March 3, 2011). "Thorium." *Toxic Substances Portal* Retrieved May 31, 2011, from <http://www.atsdr.cdc.gov/substances/toxsubstance.asp?toxid=121>.
- Baes, C. F. and R. E. Mesmer (1981). "The Thermodynamics of Cation Hydrolysis." *American Journal of Science* **281**(7): 935-962.
- Baes, C. F., N. J. Meyer and C. E. Roberts (1965). "Hydrolysis of Thorium(4) at 0 and 95 Degrees." *Inorganic Chemistry* **4**(4): 518-&.
- Banik, N. L., R. A. Buda, S. Burger, J. V. Kratz and N. Trautmann (2007). "Sorption of tetravalent plutonium and humic substances onto kaolinite." *Radiochimica Acta* **95**(10): 569-575.
- Bitea, C., R. Muller, V. Neck, C. Walther and J. I. Kim (2003). "Study of the generation and stability of thorium(IV) colloids by LIBD combined with ultrafiltration." *Colloids and Surfaces a-Physicochemical and Engineering Aspects* **217**(1-3): 63-70.
- Brown, P. L., J. Ellis and R. N. Sylva (1983). "The Hydrolysis of Metal-Ions .5. Thorium(IV)." *Journal of the Chemical Society-Dalton Transactions*(1): 31-34.
- Buda, R. A., N. L. Banik, J. V. Kratz and N. Trautmann (2008). "Studies of the ternary systems humic substances - kaolinite - Pu(III) and Pu(IV)." *Radiochimica Acta* **96**(9-11): 657-665.
- Chang, P., S. Yu, T. Chen, A. Ren, C. Chen and X. Wang (2007). "Effect of pH, ionic strength, fulvic acid and humic acid on sorption of Th(IV) on Na-rectorite." *Journal of Radioanalytical and Nuclear Chemistry* **274**(1): 153-160.
- Chen, C. L. and X. K. Wang (2007). "Influence of pH, soil humic/fulvic acid, ionic strength and foreign ions on sorption of thorium(IV) onto gamma- Al_2O_3 ." *Applied Geochemistry* **22**(2): 436-445.

- Chen, C. L. and X. K. Wang (2007). "Sorption of Th (IV) to silica as a function of pH, humic/fulvic acid, ionic strength, electrolyte type." Applied Radiation and Isotopes **65**(2): 155-163.
- Choppin, G. R. (1999). "Utility of oxidation state analogs in the study of plutonium behavior." Radiochimica Acta **85**(3-4): 89-95.
- Choppin, G. R. (2006). "Environmental Behavior of Actinides." Czechoslovak Journal of Physics **56**: D13-D21.
- Choppin, G. R. (2007). "Actinide speciation in the environment." Journal of Radioanalytical and Nuclear Chemistry **273**(3): 695-703.
- Cornell, R. M. and U. Schwertmann (2003). The Iron Oxides: Structure, Properties, Reactions, Occurrences, and Uses, Wiley-VCH.
- Cromieres, L., V. Moulin, B. Fourest, R. Guillaumont and E. Giffaut (1998). "Sorption of thorium onto hematite colloids." Radiochimica Acta **82**: 249-255.
- Degueldre, C. and A. Kline (2007). "Study of thorium association and surface precipitation on colloids." Earth and Planetary Science Letters **264**(1-2): 104-113.
- Delistraty, D. A. and J. Yokel (1999). "Ecotoxicity of riverbank spring water along the Hanford Reach, Columbia River." Environmental Toxicology **14**(5): 473-480.
- Duffo, G. S., S. B. Farina, F. M. Schulz and F. Marotta (2010). "Corrosion susceptibility of steel drums containing cemented intermediate level nuclear wastes." Journal of Nuclear Materials **405**(3): 274-279.
- Ekberg, C., Y. Albinsson, M. J. Comarmond and P. L. Brown (2000). "Studies on the complexation behavior of thorium(IV). 1. Hydrolysis equilibria." Journal of Solution Chemistry **29**(1): 63-86.
- Fan, Q. H., W. S. Wu, X. P. Song, J. Z. Xu, J. Hu and Z. W. Niu (2008). "Effect of humic acid, fulvic acid, pH and temperature on the sorption-desorption of Th(IV) on attapulgite." Radiochimica Acta **96**(3): 159-165.
- Felmy, A. R., D. Rai, S. M. Sterner, M. J. Mason, N. J. Hess and S. D. Conradson (1997). "Thermodynamic models for highly charged aqueous species: Solubility of Th(IV) hydrous oxide in concentrated NaHCO₃ and Na₂CO₃ solutions." Journal of Solution Chemistry **26**(3): 233-248.
- Freidman, H. (2011). "The Mineral Thorite." The Mineral & Gemstone Kingdom Retrieved Jun. 21, 2011, from <http://www.minerals.net/mineral/thorite.aspx>.
- Grenthe, I. and B. Lagerman (1991). "Studies on Metal Carbonate Equilibria .23. Complex-Formation in the Th(IV)-H₂O-Co₂(G) System." Acta Chemica Scandinavica **45**(3): 231-238.
- Guo, P. R., T. C. Duan, X. J. Song, J. W. Xua and H. T. Chen (2008). "Effects of soil pH and organic matter on distribution of thorium fractions in soil contaminated by rare-earth industries." Talanta **77**(2): 624-627.
- Guo, Z. J., L. J. Niu and Z. Y. Tao (2005). "Sorption of Th(IV) ions onto TiO₂: Effects of contact time, ionic strength, thorium concentration and phosphate." Journal of Radioanalytical and Nuclear Chemistry **266**(2): 333-338.
- Guo, Z. J., X. M. Yu, F. H. Guo and Z. Y. Tao (2005). "Th(IV) adsorption on alumina: Effects of contact time, pH, ionic strength and phosphate." Journal of Colloid and Interface Science **288**(1): 14-20.

- Hartzog, O. K., V. A. Loganathan, S. R. Kanel, G. R. Jeppu and M. O. Barnett (2009). "Normalization, comparison, and scaling of adsorption data: Arsenate and goethite." Journal of Colloid and Interface Science **333**(1): 6-13.
- Hunter, K. A., D. J. Hawke and L. K. Choo (1988). "Equilibrium Adsorption of Thorium by Metal-Oxides in Marine Electrolytes." Geochimica Et Cosmochimica Acta **52**(3): 627-636.
- IUPAC. (2002, Sept 05, 2002). "Definition and Classification of Colloids." Retrieved July 10, 2011, from http://old.iupac.org/reports/2001/colloid_2001/manual_of_s_and_t/node33.html.
- Jakobsson, A. M. (1999). "Measurement and modeling of Th sorption onto TiO₂." Journal of Colloid and Interface Science **220**(2): 367-373.
- Kaplan, D. I. (2010). Sediment Characterization. M. O. Barnett.
- Kim, J. S., S. K. Kwon, M. Sanchez and G. C. Cho (2011). "Geological Storage of High Level Nuclear Waste." Ksce Journal of Civil Engineering **15**(4): 721-737.
- Kim, S. S., M. H. Baik, J. W. Choi, H. S. Shin and J. I. Yun (2010). "The dissolution of ThO₂(cr) in carbonate solutions and a granitic groundwater." Journal of Radioanalytical and Nuclear Chemistry **286**(1): 91-97.
- Laflamme, B. D. and J. W. Murray (1987). "Solid-Solution Interaction - The Effect of Carbonate Alkalinity on Adsorbed Thorium." Geochimica Et Cosmochimica Acta **51**(2): 243-250.
- Li, W. J. and Z. Y. Tao (2002). "Comparative study on Th(IV) sorption on alumina and silica from aqueous solutions." Journal of Radioanalytical and Nuclear Chemistry **254**(1): 187-192.
- Mathes, S. E. and T. C. Rasmussen (2006). "Combining multivariate statistical analysis with geographic information systems mapping: a tool for delineating groundwater contamination." Hydrogeology Journal **14**(8): 1493-1507.
- Milic, N. B. (1971). "Studies on Hydrolysis of Metal Ions .61. Hydrolysis of Thorium(IV) Ion in Lithium, Potassium, and Magnesium Nitrate Media." Acta Chemica Scandinavica **25**(7): 2487-&.
- Milic, N. B. (1981). "Linear Free-Energy Relationships in the Hydrolysis of Metal-Ions - The Effect of the Ionic Medium." Journal of the Chemical Society-Dalton Transactions(7): 1445-1449.
- Murphy, R. J., J. J. Lenhart and B. D. Honeyman (1999). "The sorption of thorium (IV) and uranium (VI) to hematite in the presence of natural organic matter." Colloids and Surfaces a-Physicochemical and Engineering Aspects **157**(1-3): 47-62.
- Neck, V., M. Altmaier, R. Muller, A. Bauer, T. Fanghanel and J. I. Kim (2003). "Solubility of crystalline thorium dioxide." Radiochimica Acta **91**(5): 253-262.
- Neck, V. and J. I. Kim (2000). "An electrostatic approach for the prediction of actinide complexation constants with inorganic ligands-application to carbonate complexes." Radiochimica Acta **88**(9-11): 815-822.
- Neck, V. and J. I. Kim (2001). "Solubility and hydrolysis of tetravalent actinides." Radiochimica Acta **89**(1): 1-16.

- Neck, V., R. Muller, M. Bouby, M. Altmaier, J. Rothe, M. A. Denecke and J. I. Kim (2002). "Solubility of amorphous Th(IV) hydroxide - application of LIBD to determine the solubility product and EXAFS for aqueous speciation." Radiochimica Acta **90**(9-11): 485-494.
- Osthols, E. (1995). "Thorium Sorption on Amorphous Silica." Geochimica Et Cosmochimica Acta **59**(7): 1235-1249.
- Osthols, E., J. Bruno and I. Grenthe (1994). "On The Influence of Carbonate on Mineral Dissolution .3. The Solubility of Microcrystalline ThO₂ in CO₂-H₂O Media." Geochimica Et Cosmochimica Acta **58**(2): 613-623.
- Osthols, E., A. Manceau, F. Farges and L. Charlet (1997). "Adsorption of thorium on amorphous silica: An EXAFS study." Journal of Colloid and Interface Science **194**(1): 10-21.
- Peterson, J., M. MacDonell, L. Haroun, F. Monette, R. D. Hildebrand and A. Taboas (2007). Thorium. Radiological and Chemical Fact Sheets to Support Health Risk Analyses for Contaminated Areas. Argonne National Laboratory Environmental Science Division.
- Powell, B. A., R. A. Fjeld, D. I. Kaplan, J. T. Coates and S. M. Serkiz (2005). "Pu(V)O₂(+) adsorption and reduction by synthetic hematite and goethite." Environmental Science & Technology **39**(7): 2107-2114.
- Powell, B. A., R. A. Fjeld, D. I. Kaplan, J. T. Coates and S. M. Serkiz (2004). "Pu(V)O₂(+) adsorption and reduction by synthetic magnetite (Fe₃O₄)." Environmental Science & Technology **38**(22): 6016-6024.
- Powell, B. A., A. F. Robert, J. T. Coates, D. I. Kaplan and S. M. Serkiz (2002). Plutonium Oxidation State Geochemistry in the SRS Subsurface Environment US Department of Energy.
- Rai, D., D. A. Moore, C. S. Oakes and M. Yui (2000). "Thermodynamic model for the solubility of thorium dioxide in the Na⁺-Cl⁻-OH⁻-H₂O system at 23 degrees C and 90 degrees C." Radiochimica Acta **88**(5): 297-306.
- Rand, M., J. Fuger, V. Neck, I. Grenthe and D. Rai (2008). Chemical Thermodynamics of Thorium. Amsterdam, The Netherlands, North Holland Elsevier Science Publishers B. V.
- Reiller, P., F. Casanova and V. Moulin (2005). "Influence of addition order and contact time on thorium(IV) retention by hematite in the presence of humic acids." Environmental Science & Technology **39**(6): 1641-1648.
- Reiller, P., V. Moulin, F. Casanova and C. Dautel (2002). "Retention behaviour of humic substances onto mineral surfaces and consequences upon thorium (IV) mobility: case of iron oxides." Applied Geochemistry **17**(12): 1551-1562.
- Righetto, L., G. Bidoglio, B. Marcandalli and I. R. Bellobono (1988). "Surface Interactions of Actinides with Alumina Colloids." Radiochimica Acta **44-5**: 73-75.
- Rajo, I., F. Seco, M. Rovira, J. Gimenez, G. Cervantes, V. Marti and J. de Pablo (2009). "Thorium sorption onto magnetite and ferrihydrite in acidic conditions." Journal of Nuclear Materials **385**(2): 474-478.
- Runde, W. (2000). "The Chemical Interactions of Actinides in the Environment." Los Alamos Science **26**: 20.

- Ryan, J. L. and D. Rai (1987). "Thorium(IV) Hydrous Oxide Solubility." Inorganic Chemistry **26**(24): 4140-4142.
- Schmeide, K. and G. Bernhard (2010). "Sorption of Np(V) and Np(IV) onto kaolinite: Effects of pH, ionic strength, carbonate and humic acid." Applied Geochemistry **25**(8): 1238-1247.
- Schwertmann, U. and R. M. Cornell (2000). Iron Oxides in the Laboratory. Weinheim, Wiley-VCM.
- Seco, F., C. Hennig, J. de Pablo, M. Rovira, I. Rojo, V. Marti, J. Gimenez, L. Duro, M. Grive and J. Bruno (2009). "Sorption of Th(IV) onto Iron Corrosion Products: EXAFS Study." Environmental Science & Technology **43**(8): 2825-2830.
- Snoeyink, V. and D. Jenkins (1980). Water Chemistry. New York, Wiley.
- Tan, X. L., X. K. Wang, C. L. Chen and A. H. Sun (2007). "Effect of soil humic and fulvic acids, pH and ionic strength on Th(IV) sorption to TiO₂ nanoparticles." Applied Radiation and Isotopes **65**(4): 375-381.
- USEPA. (2011). "Thorium." Retrieved May 31, 2011, from <http://www.epa.gov/rpdweb00/radionuclides/thorium.html>.
- Vandenborre, J., A. Abdelouas and B. Grambow (2008). "Discrepancies in thorium oxide solubility values: a new experimental approach to improve understanding of oxide surface at solid/solution interface." Radiochimica Acta **96**(9-11): 515-520.
- Vasicek, R. and J. Svoboda (2011). "Long-term lining performance - Civil engineering problem of potential retrieval of buried spent nuclear fuel." Nuclear Engineering and Design **241**(4): 1233-1237.
- Yun, J. I., M. A. Kim, P. J. Panak, J. I. Kim and T. Fanghanel (2006). "Formation of aquatic Th(IV) colloids and stabilization by interaction with Cm(III)/Eu(III)." Journal of Physical Chemistry B **110**(11): 5416-5422.

Appendix

The following calculations were used to determine the results shown in the figures from Chapter 3.

Dissolved Th(IV) Concentration, C

Example

Given: Concentration from ICP analysis, $C_{ICP} = 6.789 \text{ mg/L}$, Molecular weight of thorium, $MW_{Th} = 232.04 \text{ g/mol}$. Each sample was acidified to 5% 2M HNO_3 : Vial weight, $W_v = 4.073 \text{ g}$, Vial + Solution Weight, $W_{v+s} = 9.811 \text{ g}$, Total Sample Weight, $W_t = 10.130$

Step 1: Dissolved Th(IV) Concentration in mg/L

$$C_f = C_{ICP} \left(\frac{W_t - W_v}{W_{v+s} - W_v} \right) = 6.789 \text{ mg/L} \cdot \left(\frac{10.130 \text{ g} - 4.073 \text{ g}}{9.811 \text{ g} - 4.073 \text{ g}} \right) = 7.166 \text{ mg/L}$$

Step 2: Convert to $\mu\text{mol/L}$ (μM)

$$C_f = \frac{C}{MW} = \frac{7.166 \text{ mg/L}}{232.04 \text{ g/mol}} \cdot \left(\frac{1 \text{ g}}{1000 \text{ mg}} \right) \cdot \left(\frac{10^6 \mu\text{mol}}{1 \text{ mol}} \right) = 30.88 \mu\text{M}$$

Step 3: Determine pC

$$pC = -\log(C_f) = -\log(30.88 \mu\text{M}) = -1.49$$

Th(IV) Uptake, q

Example

Given: Total sample volume, $V_t = 30.112$, Volume of Th(IV) stock solution in sample, $V_{Th} = 0.217$, Concentration of Th(IV) stock solution, $C_{stock} = 1025 \text{ mg/L}$, Dissolved Th(IV) concentration of sample, $C_f = 7.166 \text{ mg/L}$, Mass of soil in sample, $m = 0.0152 \text{ g}$

Step 1: Initial aqueous Th(IV) concentration, C_0

$$C_0 = \frac{C_{stock} \cdot V_{Th}}{V_t} = \frac{1025 \text{ mg/L} \cdot 0.217 \text{ mL}}{30.112 \text{ mL}} = 7.400 \text{ mg/L}$$

Step 2:

Th(IV) concentration adsorbed to geomeia, q

$$q = \frac{(C_0 - C_f) \cdot V_t}{1000 \cdot m} = \frac{(7.400 \text{ mg/L} - 7.166 \text{ mg/L}) \cdot 30.112 \text{ mL}}{1000 \text{ mL/L} \cdot 0.0152 \text{ g}}$$

$$q = 0.4636 \frac{\text{mg}}{\text{g}} \cdot \left(\frac{1000 \text{ } \mu\text{g/mg}}{232.04 \text{ } \mu\text{g}/\mu\text{mol}} \right)$$

$$q = 1.998 \text{ } \mu\text{mol/g}$$

% Th(IV) Dissolved in solution

Example

Given: Total sample volume, $V_t = 30.112$, Dissolved Th(IV) Concentration, $C_f = 7.166$ mg/L, Initial sample Th(IV) concentration, $C_0 = 7.400$ mg/L

Step 1:

Total mass of thorium in sample, m_t

$$m_t = \frac{C_0 \cdot V_t}{1000 \text{ mL/L}} = \frac{7.400 \text{ mg/L} \cdot 30.112 \text{ mL}}{1000 \text{ mL/L}} = 0.223 \text{ mg}$$

Step 2:

Mass of thorium dissolved in solution, m_d

$$m_d = \frac{C_f \cdot V_t}{1000 \text{ mL/L}} = \frac{7.166 \text{ mg/L} \cdot 30.112 \text{ mL}}{1000 \text{ mL/L}} = 0.216 \text{ mg}$$

Step 3:

% Th(IV) Dissolved in solution

$$\% = \frac{m_d}{m_t} \cdot 100\% = \frac{0.216 \text{ mg}}{0.223 \text{ mg}} \cdot 100\% = 96.86\%$$

Particle size removed – Stoke's Law

Example

Given: Radius of rotation of the top of the sediment, $R = 12.4$ cm, Radius of rotation of the surface of the suspension in the tube, $S = 6.1$ cm, Centrifugation speed, $N_m = 8000$ rpm, Centrifugation time, $t_{\min} = 30$ minutes, Viscosity of liquid @ 25°C (poise), $\eta = 0.0089$ g/cm-s, Density of the solid (ThO₂), $\rho_{Th} = 10$ g/cm³, Density of the liquid (H₂O), $\rho_w = 1$ g/cm³, Density of the solid (soil), $\rho_s = 2.65$ g/cm³

Step 1:

Size of Th(IV) solid removed

$$D_{\mu m} = \sqrt{\frac{63.0 \times 10^8 \eta \log\left(\frac{R}{S}\right)}{N_m^2 \cdot t_{\min} \cdot (\rho_{Th} - \rho_w)}} = \sqrt{\frac{63.0 \times 10^8 \cdot 0.0089 \text{ g/cm} \cdot \text{s} \cdot \log\left(\frac{12.4 \text{ cm}}{6.1 \text{ cm}}\right)}{(8000 \text{ min}^{-1})^2 \cdot 30 \text{ min} \cdot (10 \text{ g/cm}^3 - 1 \text{ g/cm}^3)}$$

$$D_{\mu m} = 0.032 \text{ } \mu\text{m}$$

Step 2: Size of soil particle removed

$$D_{\mu m} = \sqrt{\frac{63.0 \times 10^8 \eta \log\left(\frac{R}{S}\right)}{N_m^2 \cdot t_{\min} \cdot (\rho_{Th} - \rho_w)}}$$

$$D_{\mu m} = \sqrt{\frac{63.0 \times 10^8 \cdot 0.0089 \text{ g/cm} - s \cdot \log\left(\frac{12.4 \text{ cm}}{6.1 \text{ cm}}\right)}{(8000 \text{ min}^{-1})^2 \cdot 30 \text{ min} (2.65 \text{ g/cm}^3 - 1 \text{ g/cm}^3)}}$$

$$D_{\mu m} = 0.074 \mu m$$